SEMMELWEIS EGYETEM

DOKTORI ISKOLA

Ph.D. értekezések

2904.

RÓKA BEÁTA

A folyadék- és elektrolitháztartás szabályozásának élet- és kórélettana-Keringés és vérnyomás szabályozás
című program

Programvezető: Dr. Zsembery Ákos, egyetemi docens

Témavezetők: Dr. Hamar Péter, egyetemi tanár
Dr. Szénási Gábor, tudományos főmunkatárs

TIME-DEPENDENT miRNA PROFILE AND RENAL ACUTE PHASE RESPONSE DURING SEPTIC ACUTE KIDNEY INJURY IN MICE

PhD thesis

Beáta Róka

Doctoral School of Theoretical and Translational Medicine

Semmelweis University

Supervisors:	Péter Hamar, MD, DSc
	Gábor Szénási, CSc
Official reviewers:	Ádám Hosszú, MD, PhD
	Béla Nagy, MD, PhD

Head of the Complex Examination Committee: István Karádi, MD, DSc

Members of the Complex Examination Committee:

Lívia Jánoskuti, MD, PhD

József Borbola, MD, PhD

Budapest

2023

Table of Contents

List of Abbreviations

A1AGP	α-1-acid glycoprotein
A2m	alpha-2-macroglobulin
AKI	acute kidney injury
Alb	serum albumin
ANOVA	analysis of variance
ApoA1	apolipoprotein A1
ApoE	apolipoprotein E
APP	acute-phase protein
APR	acute-phase response/reaction
Aqp1	aquaporin-1
B2m	beta-2-microglobulin
C3	complement C3
Chil3	chitinase-like protein 3
Cp	ceruloplasmin
DAMP	damage associated molecular pattern
DBP	vitamin D-binding protein
DTT	dithiothreitol
EP	early phase
FC	fold change
Fga	fibrinogen-α
Fgb	fibrinogen-β
Fgg	fibrinogen-γ
FHC	ferritin heavy chain
Gapdh	Glyceraldehyde 3-phosphate dehydrogenase
GEO	Gene Expression Omnibus
Hp	haptoglobin
HPLC	High Performance Liquid Chromatography
Hpx	hemopexin
IL-6	interleukin-6
Itih1	inter alpha-trypsin inhibitor heavy chain 1

Itih4	inter alpha-trypsin inhibitor heavy chain 4
KO	knock-out
Lcn-2	lipocalin-2
LFQ	label-free quantification
LP	late phase
LPS	lipopolysaccharide
min	minute
miR	microRNA
miRNA	microRNA
miRNome	transcriptome of miRNAs
mRNA	messenger RNA
MS	mass spectrometry
MOF	multiple-organ failure
NBCe1	electrogenic sodium bicarbonate cotransporter 1
NCBI	National Center for Biotechnology Information
NGAL	neutrophil gelatinase-associated lipocalin
Oat3	organic anion transporter 3
PRP	pattern-recognition receptor
qPCR	quantitative polymerase chain reaction
Saa	serum amyloid A
Sar1b	secretion associated Ras related GTPase 1B
SD	standard deviation
SDS	sodium dodecyl sulfate
SDS-PAGE	sodium dodecyl sulfate–polyacrylamide gel electrophoresis
SEM	standard error of the mean
Serpina1	alpha-1-antitrypsin
Serpina3k	serine protease inhibitor A3K
Serpina3n	serine protease inhibitor A3N
Slc22a8	solute carrier family 22 member 8
Slc4a4	solute carrier family 4 member 4
Tf	transferrin
TLR	toll-like receptor

TNF-α	tumor necrosis factor-α
Tris	tris(hydroxymethyl)aminomethane
Vwa5a	von Willebrand factor A domain-containing protein 5A

1. Introduction

Sepsis is one of the leading causes of critical illness and mortality with constantly increasing incidence (1,2). Sepsis is a severe and potentially life-threatening organ dysfunction induced by a dysregulated immune response to an infection, leading to circulatory shock with consequent multiple-organ failure (MOF) (3,4). Acute kidney injury (AKI) can develop with a high incidence in septic patients (5), making sepsis one of the most common aetiologies of AKI (6). About half of the AKI cases is caused by severe sepsis in intensive care units associated with a 50-60% mortality rate (5). Surviving patients have an increased risk for developing chronic kidney disease and end-stage renal failure after AKI (4). Thus, there is an unmet need to treat septic AKI, and prevent the long-term deterioration of renal function and progression to renal failure. Detailed analysis of the mechanisms can be a fruitful approach to identify possible targets of intervention.

AKI is defined as an abrupt decrease in renal function. Septic shock is accompanied by reduced renal blood flow and/or microvascular dysfunction leading to kidney hypoxia, which is a major mechanism of renal damage leading to AKI. Bacterial toxins and immune stimulation also contribute to AKI development (7).

There are several animal models of sepsis one of the most popular of which is achieved by intraperitoneal injection of Gram-negative bacterial cell wall endotoxin or lipopolysaccharide (LPS). LPS injection induces a toxic state and hyperdynamic circulatory shock, modelling septic shock (8,9). Both tissue hypoxia and sepsis activate the immune system. (10) LPS is a strong and well-characterized immunostimulant (11) that triggers a systemic inflammatory response accompanied by an increased expression of pro-inflammatory cytokines (e.g. TNF-α and IL-6) (12). Immune activation is largely responsible for the vasodilation and the development of circulatory shock leading to MOF. MOF development depends on the LPS dose, thus, lethal and sub-lethal doses can be defined (13). LPS administration is an established model to study the circulatory and inflammatory effects of sepsis in various animal species including rodents (8,9). LPS-injected mice develop AKI as demonstrated previously in a number of studies (14–18) and also in our experiments (19,20) discussed in this thesis.

Renal tubular cells are exposed to inflammatory mediators secreted in response to activation by damage- (danger-) and pathogen-associated molecular patterns (DAMPs,

PAMPs). DAMPs are released from cells in response to cell damage, and activate pattern recognition receptors (PRRs), such as toll-like receptors (TLRs). Renal tubular cells produce cytokines locally (e.g. TNF-α, IL-6) upon TLR activation. PAMPs are small molecular motifs characteristic of various pathogens (e.g. LPS) and are also recognized by PRRs (5,7,10).

A well-known consequence of sepsis is the induction of the acute-phase response/reaction (APR) due to tissue damage and infection. Proteins are termed acute-phase proteins (APPs) if their plasma concentration changes by at least 25% during inflammation (21–23). Cytokines secreted during the inflammatory process increase or suppress the synthesis of APPs. Their main role is restoring homeostasis after inflammation (22). APPs are known to be principally produced and secreted into the blood stream by the liver. However, they are also synthesized in other organs and tissues, thereby contributing to local defence and facilitating tissue repair (23).

Plasma concentrations of certain APPs, such as C-reactive protein, are routinely used inflammatory markers for the diagnosis and follow-up of sepsis (24). Another APP, lipocalin-2 (Lcn-2), also named neutrophil gelatinase-associated lipocalin (NGAL), is a sensitive marker of renal tubular injury (25–28). However, these biomarkers are neither specific for sepsis nor for AKI (24,29). Serum Lcn-2 concentrations are also increased in other pathological conditions, such as gastrointestinal (30,31) and cardiovascular (32) diseases. Although numerous other AKI biomarker candidates have been identified (29,33), the various types of AKI cannot be differentiated with satisfactory specificity and sensitivity by these biomarkers (12,29). Hence, appropriate biomarkers or biomarker combinations are intensively sought for the early detection and monitoring of septic AKI (29).

Enhanced renal production of some APPs, such as fibrinogen (34), serum amyloid A (35,36), α-1-acid glycoprotein (35), ceruloplasmin (35), haptoglobin (36–38), hemopexin (39), complement C3 (40,41), beta-2-microglobulin (34) and plasminogen activator inhibitor-1 (42) have been described in septic AKI, while mRNA expression of serum albumin was shown to be reduced in the kidney (43). Although these scarce and isolated findings demonstrate that some APPs are produced in the kidney during sepsis, a coordinated, complex renal APR has not yet been evaluated.

Expression of proteins in response to inflammation is modulated by microRNAs (miRNA/miR), which are small non-coding RNAs that regulate posttranscriptional gene expression mainly via translational repression. One miRNA can bind to numerous mRNAs, and one mRNA can be affected by several miRNAs. In this way, miRNAs extensively regulate many cellular processes, such as apoptosis, cell-cycle progression and cellular differentiation (44). MiRNAs also have a great influence on complex pathological processes, such as AKI (45). MiRNAs can serve both as biomarkers and tools in the treatment of AKI (46).

A few miRNAs have been associated previously with LPS effects in the kidney including miR-21, miR-146a and miR-223 (47–52). The function of miR-223 has been best characterized. MiR-223 played a model-specific role in the kidney during experimental sepsis (51). The organ-specific effects of miRNAs can be influenced by the activity of other regulatory factors and the functional status of the cells , which can potentially result in harmful or protective effects.

2. Objectives

Our aim was to study the temporal changes in the expression of miRNAs and proteins during LPS-induced AKI in mice in order to identify miRNAs and proteins that have not yet been related to the mechanisms of septic AKI. We aimed to measure the effects of LPS on the transcriptome of miRNAs (miRNome) by miRNA microarray at four time points, i.e. 1.5 and 6 hours (early phase, EP) and 24 and 48 hours (late phase, LP) after treatment, and to confirm the microarray results by quantitative PCR (qPCR). In parallel, we also planned to measure the renal proteome changes using high performance liquid chromatography and mass spectrometry (HPLC-MS/MS). Finally, we sought to find relationships between the changes in miRNome and proteome.

3. Methods

3.1. Mice

Male Naval Medical Research Institute (NMRI) mice, weighing 25-30g, were used (Toxi-Coop, Budapest, Hungary). The animals were housed under standard conditions and had free access to tap water and standard rodent chow (Akronom Kft., Budapest, Hungary) *ad libitum*. All protocols for the animal studies were approved by the Animal Ethics Committee of Semmelweis University and the Pest County Government Office (No: XIV-1-001/2101-4/2012, XIV-1-001/2104-4/2012, XIV-1-001/2013-4/2012 and PE/EA/2202-5/2017).

3.2. Endotoxin preparations and injection

Mice were injected intraperitoneally (i.p.) with LPS from *Escherichia coli* (*E. coli*) (0111:B4; Sigma-Aldrich, Budapest, Hungary) at the doses of 10 or 40 mg/kg bodyweight (BW). Based on our previous experiments the doses were maximal, which ensured the induction of septic shock without lethality during the follow-up period (13,18). Two time points represented the early phase (EP, 1.5 h and 6 h), and two others represented the late phase (LP, 24 h and 48 h) of LPS-induced inflammation and AKI (53). Mice were divided into four treatment groups as follows:

- Group 1 (EP1.5h): sacrificed 1.5 h after injection with LPS at 40 mg/kg BW (n=7)
- Group 2 (EP6h): sacrificed 6 h after injection with LPS at 40 mg/kg BW (n=7)
- Group 3 (LP24h): sacrificed 24 h after injection with LPS at 10 mg/kg BW (n=7)
- Group 4 (LP48h): sacrificed 48 h after injection with LPS at 10 mg/kg BW (n=7)

LPS was dissolved in sterile saline immediately before use.

Mice serving as negative controls were injected i.p. with equal volume of saline in both the EP and LP settings (n=7).

3.3. Plasma and organ collection

First 5500 IU/kg BW heparin (Ratiopharm GmbH, Ulm, Germany) was administered to mice for anticoagulation. Mice were sacrificed by cervical dislocation 3 minutes (min) later. After opening their chest, blood was drawn from the transected vena cava. The collected blood was centrifuged at 6000 g for 2 min to obtain plasma samples. The animals were then transcardially perfused with physiological saline (10 ml, 4°C).

After the perfusion the kidneys were taken out, the renal capsule was removed and the organ was cut into pieces. From each kidney one piece was placed in 0.5 ml TR 118 TRI Reagent (Molecular Research Center, Inc., Cincinnati, OH, USA). This piece in the TRI Reagent and the remaining native kidney parts were all snap frozen in liquid nitrogen. Then they were stored at -80°C for molecular and proteomic analysis.

For control purposes livers of intact NMRI mice were also collected similarly.

3.4. Plasma urea determination

An enzymatic assay containing urease and glutamate-dehydrogenase (Diagnosticum Zrt., Budapest, Hungary) was used to measure plasma urea concentrations with colorimetric detection according to the manufacturer's protocol. In brief, the plasma samples were mixed with the reagent containing urease and glutamate-dehydrogenase. The assay is based on the conversion of NADH into NAD that was detected photometrically at 340 nm. A standard curve was established to calculate the urea concentration in the samples.

3.5. Total RNA extraction and reverse transcription

TRI Reagent (Molecular Research Center) was used for the extraction of total RNA according to the manufacturer's protocol. In brief, phase separation was performed with chloroform. Then the supernatants were aspirated and mixed with isopropyl alcohol to precipitate RNA. RNA was sedimented with centrifugation and the pellets were washed twice with 70% ethanol. Then the RNA pellets were dissolved in RNase-free water (AccuGENE^{TM} Molecular Biology Water, Lonza, Basel, Switzerland). RNA integrity was checked by electrophoretic separation on 1% agarose gel. RNA concentrations and purity were determined with Nanodrop 2000c Spectrophotometer (Thermo Fisher Scientific, Wilmington, DE, USA).

One μg total RNA was reverse transcribed into cDNA using the High-Capacity cDNA Archive Kit (Applied Biosystem, Foster City, CA, USA) with random hexamer primers according to the manufacturer's protocol.

3.6. MiRNA microarray profiling

Four representative samples from each test group were selected based on the IL-6, Lcn-2 and Tnf-α mRNA expression levels. Sample selection was done in a way to ensure

similar mean and standard deviation (SD) of the mRNA expression values in the four samples and the entire group.

Microarray measurements were performed by Exiqon A/S (Vedbæk, Denmark). Briefly, total RNA quality was determined with an Agilent 2100 Bioanalyzer. The miRCURY LNA™ microRNA Hi-Power Labeling Kit (Exiqon) was used for fluorescent labelling of RNA. Hy3™ and Hy5™ labels were applied on 750 ng total RNA from each test sample and the pooled reference samples. The hybridization was carried out on miRCURY LNA™ microRNA Array slides using a Tecan HS4800™ hybridization station (Tecan, Grödig, Austria) and according to the miRCURY LNA™ microRNA Array Instruction manual. After hybridization Agilent G2565BA Microarray Scanner System (Agilent Technologies, Inc., USA) was used to scan the slides. The scanned images were analyzed with the ImaGene® 9 software (miRCURY LNA™ microRNA Array Analysis Software, Exiqon). The quantified signals were background corrected using the Normexp method (offset value 10) and normalized with the global Locally Weighted Scatterplot Smoothing (Lowess) regression algorithm. The discussed microarray data were deposited in the Gene Expression Omnibus (GEO) of National Center for Biotechnology Information (NCBI) (54) and can be accessed via accession ID GSE139919 (https://www.ncbi.nlm.nih.gov/geo/query/acc.cgi?acc=GSE139919).

3.7. MiRNA qPCR

The microarray results were validated by performing qPCR in all samples. The top four most upregulated miRNAs in all groups were verified by qPCR. In addition, miR-223-3p was also measured by qPCR because various publications suggested its involvement in septic AKI as discussed in the Introduction.

Total RNA was transcribed into cDNA using the Applied Biosystem™ TaqMan™ Advanced miRNA cDNA Synthesis Kit (Applied Biosystem) according to the manufacturer's protocol. The miRNA expression levels were determined with TaqMan™ Advanced miRNA Assay (Applied Biosystem) according to the manufacturer's protocol. Relative expressions were calculated using the $2^{-\Delta\Delta Ct}$ method. Using NormFinder software (MOMA – Department of Molecular Medicine, Aarhus, Denmark) let-7g-5p miRNA was chosen with a stability value of 0.057 as reference miRNA for normalization of the microarray results (55).

3.8. Tissue homogenization for mass spectrometry

The four most representative kidney samples from each treatment group and four control kidney samples were processed for mass spectrometry (MS) analysis according to a previously described protocol (56) with slight modifications. Frozen kidney tissues were cut into approximately 30 mg pieces on dry ice without thawing. Then 8 µl lysis buffer / mg tissue was added to each piece. The lysis buffer contained 1% NP-40 lysis buffer (Roche, Basel, Switzerland), 150 mM sodium chloride (Thermo Fisher Scientific, San Jose, CA, USA), 50 mM Tris (pH 8.0, SERVA Electrophoresis GmbH, Heidelberg, Germany), 1% protease inhibitor cocktail (Sigma-Aldrich), 0.5% sodium deoxycholate (Sigma-Aldrich), 1 mM EDTA (SERVA) and 0.1% sodium dodecyl sulfate (Pierce Chemical, Dallas, TX, USA). Tissue homogenization was performed first using Dounce homogenizer, and then by passing through the tissue a 22G (0.7 mm x 38 mm) syringe needle 20 times for further homogenization. Next, the samples were gently shaken on ice for 30 min with Rotamax 120 (Heidolph Instruments GmbH, Schwabach, Germany). The supernatant was separated by centrifugation (16000 g, 10 min). Then Bradford assay (Bio-Rad Laboratories, Inc., Hercules, California, USA) was used to determine the protein concentration. 150 µg of total protein was taken from each sample and was incubated at 95°C for 5 min with a loading buffer (10mM Tris pH 6.8 (SERVA); 7.8% glycerol (CARLO ERBA Reagents, Val de Reuil, France); 0.2% sodium dodecyl sulfate (SDS) (Pierce Chemical); 0.01% Bromphenol blue (Sigma-Aldrich)) containing 10mM dithiothreitol (DTT) (Fluka Biochemica, Steinheim, Germany). Finally the samples were stored frozen until further processing.

3.9. Sample preparation for mass spectrometry

Sample preparation for HPLC-MS/MS analysis was carried out as described before (57). In brief, the earlier prepared 150 µg of total protein from each sample was separated by electrophoresis on a 12.5% SDS-PAGE gel (Lonza, Switzerland). The gel was then stained with Comassie brilliant blue and each protein lane was cut into six bands. The gel pieces were destained with 25 mM ammonium bicarbonate dissolved in 50% acetonitrile, and were washed with acetonitrile. Then they were vacuum dried and rehydrated in reducing solution (10 mM DTT (Fluka Biochemica), 25 mM ammonium bicarbonate). The rehydrated gel pieces were incubated at 56°C for 45 min. Following this the solution was exchanged to alkylating solution containing 55 mM iodoacetamide (Amersham

Biosciences, Little Chalfont, UK) and 25 mM ammonium bicarbonate. After a 30-min of incubation at room temperature in the dark, the gel pieces were washed with acetonitrile. Then they were again vacuum dried and rehydrated in 80 µl of trypsinization buffer (25 mM ammonium bicarbonate) containing 1 µg of modified porcine trypsin (sequencing-grade, Promega, Madison, WI, USA). They were incubated at 37°C overnight. The trypsin solution was collected afterwards. The gel pieces were treated with extraction solution (50% acetonitrile, 5% formic acid (JT Baker)) to extract the remaining peptides. The extraction solution and the trypsin solution were mixed and concentrated by vacuum drying to a final volume of about 20 µl.

3.10. Mass spectrometry analysis

HPLC-MS/MS analysis was carried out using an EASY-nanoLC II HPLC unit (Thermo Fisher Scientific) and an Orbitrap LTQ Velos mass spectrometer (Thermo Fisher Scientific). The previously prepared samples that contained 0.1% formic acid were loaded onto a C18 trapping column (Proxeon Easy-column, Thermo Fischer Scientific). Separation was done by a C18 PicoFrit Aquasil analytical column (New Objective). Peptide elution was done at a constant flow rate of 0.3 µl/min in a 5–40% (v/v) linear gradient of acetonitrile (0.1%) and formic acid solution over 90 min. The full MS mass spectra were acquired in the mass range of 300 to 2,000 m/z at resolution of 30,000 (Orbitrap mass analyzer). The nine most intense precursor ions in the MS/MS spectra were obtained by Higher-energy C-trap dissociation fragmentation and recorded at a resolution of 7,500 if the charge state was above one (> 1). The dynamic exclusion was set to repeat count of 1, repeat duration of 30 s, and exclusion duration of 20 s.

3.11. Analysis of mass spectrometry data

Data analysis was a repetition of our previously published method (57) with minor modifications. MaxQuant proteomics software (version 1.6.0.13) was used for database search and quantification by spectral counting (58). Mus musculus Uniprot database search was performed (database date 15.10.2017, 16923 entries). Methionine oxidation (+15.995 Da) and protein N-terminal acetylation (+45.011 Da) were set as variable modifications. Carbamido-methylation of cysteines (+57.021 Da) was set as fixed modification. Trypsin cleavage after arginine and lysine was used as the enzyme specificity. For database searches one missed cleavage was allowed. In addition,

precursor ion and fragment ion mass tolerances were set to 20 ppm and 0.5 Da, respectively. A reversed database search was performed and the false discovery rate was set at 1% for peptide and protein identifications. Raw data and database search files can be accessed via ProteomeXchange with identifier PXD014664 (59). Relative quantification of identified proteins was performed by label-free quantification (LFQ) algorithm in MaxQuant.

3.12. MiRNA target prediction

The MirTarbase (60) and previous publications were searched for proteins that could be targets of the significantly dysregulated miRNAs in our experiment, and had been identified with strong evidence or had been validated. Predicted targets of these miRNAs were obtained from miRDB (61,62) and microRNA.org (63).

MS results were then checked against the lists of the predicted and validated targets of the miRNAs.

3.13. qPCR analysis of gene expression

Gene expression was measured by qPCR in the mouse kidney. Tnf-α and IL-6 mRNA expression levels were determined to assess the degree of LPS-induced inflammation in the kidneys. Renal tubular damage was assessed by Lcn-2 gene expression. Furthermore, renal gene expression of MS-identified APPs was measured. Glyceraldehyde 3-phosphate dehydrogenase (Gapdh) was used as an endogenous reference gene.

Primers (Table 1) were designed using NCBI/Primer-BLAST online software with one exception. Primers for Serpina1 were adapted from Zager et al. (64). Primers were synthesized by Integrated DNA Technologies Inc. (Coralville, IA, USA). Primers of APPs were tested on normal liver samples as positive control.

Gene expression in kidney tissue homogenates was determined on Bio-Rad C1000™ Thermal Cycler with CFX96™ Optics Module real-time PCR system (Bio-Rad Laboratories, Inc.). SensiFAST™ SYBR No-ROX Kit (Bioline Reagents Limited, London, UK) was used for the qPCR reaction, according to the manufacturer's protocol. Primer annealing was carried out at 60°C. Measurements were performed in duplicates. The relative quantification ($\Delta\Delta C$q) method was applied to calculate expression. The efficiency of the qPCR reaction was verified with standard curves, while the melting

curve was checked to assess the quality of the PCR product. Expression was considered to be below the limit of detection when no specific amplificon was present in the samples.

Table 1. Sequences of primers used for qPCR. Alb: serum albumin, C3: complement C3, Chil3: chitinase-like protein 3, Cp: ceruloplasmin, Gapdh: glyceraldehyde 3-phosphate dehydrogenase, Fga: fibrinogen-α, Fgb: fibrinogen-β, Fgg: fibrinogen-γ, FHC: ferritin heavy chain, Hp: haptoglobin, Hpx: hemopexin, IL-6: interleukin-6, Itih4: inter alpha-trypsin inhibitor heavy chain 4, Lcn-2: lipocalin-2, Saa: serum amyloid A, Serpina1, Serpina1a, Serpina1c: alpha-1-antitrypsin and isoforms a and c, Serpina3k: serine protease inhibitor A3K, Tf: transferrin, Tnf- α: tumor necrosis factor-α.

Target	Forward primer	Reverse primer
Alb	TTGGCAACAGACCTGACCAA	GTGTCATGCTCCACCTCACT
C3	ATCCAGACAGACCAGACCATCT	AGGATGACGACTGTCTTGCC
Chil3	AGAAGCTCTCCAGAAGCAATCC	TCAGCTGGTAGGAAGATCCCA
Cp	AGGCCCTGATGAGGAACATCT	TGCTGTGAGGAGCGACCT
Gapdh	CCAGAATGAGGATCCCAGAA	ACCACCTGAAACATGCAACA
Fga	TGAGCCATCCCTAAACGCAG	GCCAGTCTGAGTCCTTGCAT
Fgb	GGCTTCACGGTACAGAACGA	ATTTGGATTGGCTGCATGGC
Fgg	ATGAACAAATGTCACGCAGGC	TCAACTTCATGATCCACGCTGA
FHC	CCCTTTGCAACTTCGTCGTTC	GAGCCACATCATCTCGGTCAA
Hp	GTGGAGCACTTGGTTCGCTA	CCATAGAGCCACCGATGATGC
Hpx	CGCTACTACTGCTTCCAGGG	AGCTATGCCATCCATCACGG
IL-6	GATGCTACCAAACTGGATATAATC	GGTCCTTAGCCACTCCTTCTGTG
Itih4	TCCGTTGCAGCACAATATCCT	TCACTTCGAGCCACGAGAAC
Lcn-2	AGGTGGTACGTTGTGGGC	CTGTACCTGAGGATACCTGTG
Saa	GCAGGATGAAGCTACTCACCA	TGGTCAGCAATGGTGTCCTC
Serpina1	TTCCAACACCTCCTCCAAAC	CACCGCCTCAGCTATCTTTC
Serpina1a	TCAATTCAGTGTCCTCTCCAGC	AAGTCTCCCAGGTTTGTAGCG
Serpina1c	CCAGAAGGTTAGCCCAGATCCAC	GGCATAGAATAAGGAACGGCTAGT
Serpina3k	CAGCAGGACAGATTCCAGCC	AGGAGTCAGCTATCACAGAGGC
Tf	CCCAAGGATGGACTACAGGC	TGATGCTCCACTCGTCACAC
Tnf-α	AAATGGCCTCCCTCTCATCA	AGATAGCAAATCGGCTGACG

3.14. Statistics

Unless otherwise stated, continuous variables are shown as mean±standard error of the mean (SEM).

We used the ROUT method to detect possible outliers (65) (ROUT method is a combination of robust nonlinear regression and an outlier identification method to identify and remove outliers) (significance was set at p=0.01). Outliers identified were omitted from the analysis. One-way analysis of variance (ANOVA) followed by Tukey's multiple comparisons test was used for between-group comparisons. The Kruskal–Wallis one-way analysis of variance by ranks was used followed by Dunn's test if Bartlett's test indicated heterogeneity of variances. Two groups were compared by the unpaired Student's t-test. The null hypothesis was rejected if $p < 0.05$.

MiRNAs were considered to be differentially expressed with significant fold changes (FCs) above 1.5 or below 0.75 in the miRNA microarray analysis. FCs were calculated as the ratio of the means of the treated and control groups. Only miRNAs with an average Hy3 signal intensity above 6.0 were included in the analysis.

FCs of messenger RNA and miRNA (in qPCR assays) were calculated as the ratio of each normalized expression value to the mean of the respective control group, and, for statistical analysis, the data were log10 transformed in qPCR assays. The expression values of one mouse were excluded from the statistical analysis in the LP48h group, because most of its mRNA expression values were identified as outliers (ROUT test).

LFQ intensity values were log2 transformed for statistical analysis. Protein FC values were calculated as the ratio of the means of the treated and control groups (log_2FC).

Graphs were created and statistical analyses were performed using GraphPad Prism (version 6.01 and version 8.0.2, GraphPad Software Inc, San Diego, CA, USA).

4. Results

4.1. LPS-induced severe renal inflammation

All animals survived in the EP1.5h and EP6h groups (injected with 40 mg/kg LPS) but one mouse died in both the LP24h and LP48h groups (injected with 10 mg/kg LPS).

Endotoxin significantly upregulated the mRNA expression of tumour necrosis factor-α (Tnf-α) and interleukin-6 (IL-6) in the kidney in both the early and late phases and at all four time points (Fig. 1). Both LPS doses induced severe renal inflammatory responses. IL-6 mRNA expression started to decrease at 48 hours.

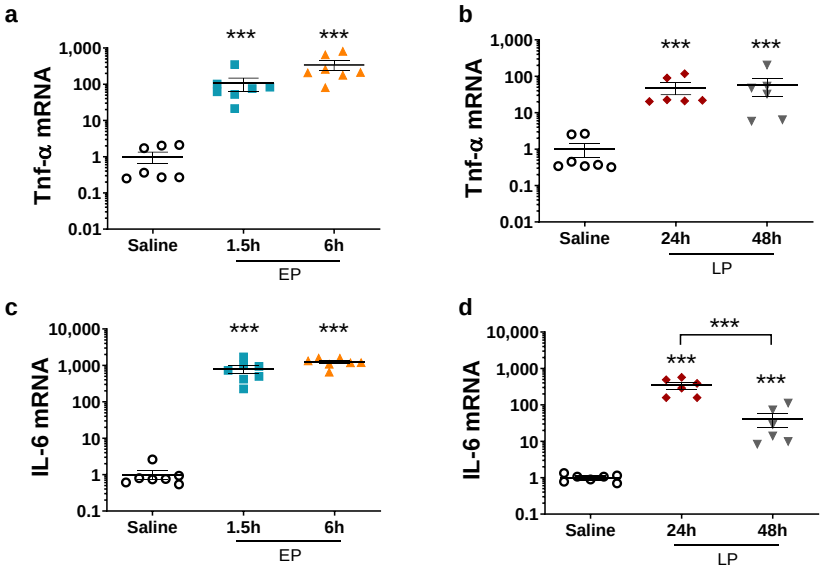

Figure 1. Relative mRNA expression of pro-inflammatory proteins after LPS injection normalized to Gapdh (fold changes vs. saline). (a, b) Tnf-α mRNA (a) EP, 1.5 h and 6 h, (b) LP, 24 h and 48 h, (c, d) IL-6 mRNA (c) EP, 1.5 h and 6 h, (d) LP, 24 h and 48 h. Data are expressed as mean ± SEM; One-way ANOVA and Dunnett's post hoc test; ***: $p<0.001$ (19)

4.2. LPS-induced renal tubular damage

Plasma urea concentrations increased first at 6 hours after endotoxin administration, increased further at 24 hours, and started to decline at 48 hours (Fig. 2/a,b). LPS significantly upregulated renal expression of Lcn-2 mRNA and protein already from 1.5 hours and from 6 hours, respectively (Fig. 2/c-f). Increased plasma urea concentrations and Lcn-2 expression indicated impaired renal function and ongoing, acute tubular injury,

respectively. The decrease in plasma urea concentrations and Lcn-2 mRNA at 48 h indicated that septic AKI was transient in our experiment.

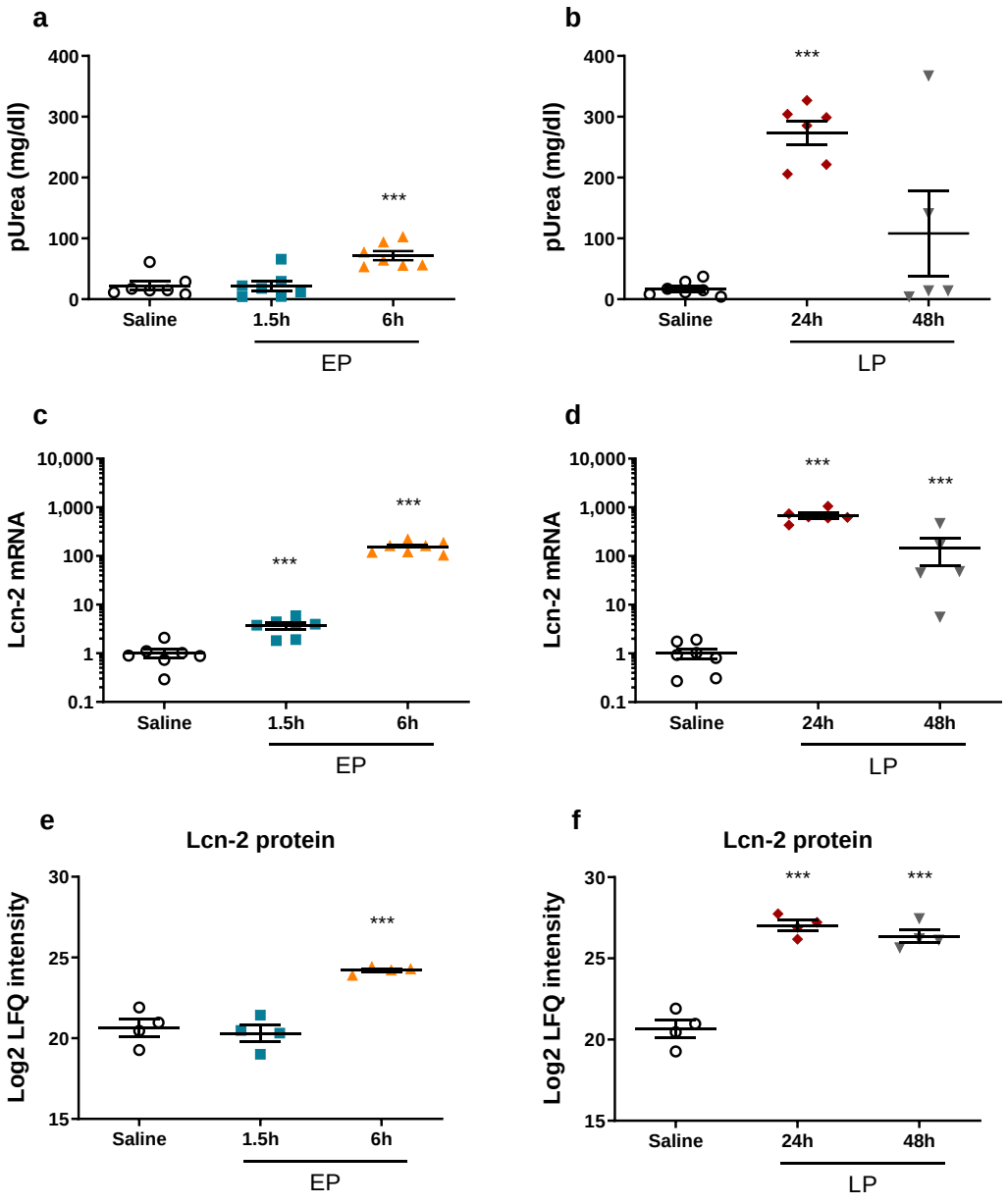

Figure 2. Markers of kidney injury after LPS administration. (a, b) Plasma urea concentration, (a) EP, 1.5 h and 6 h, (b) LP, 24 h and 48 h; (c, d) Lcn-2 mRNA expression normalized to Gapdh (fold changes vs. saline), (c) EP, 1.5 h and 6 h, (d) LP, 24 h and 48 h; (e, f) label-free quantification (LFQ) intensity values (relative amount) of Lcn-2 protein measured by HPLC-MS/MS, (e) EP, 1.5 h and 6 h, (f) LP, 24 h and 48 h. Data are

expressed as mean ± SEM; One-way ANOVA and Dunnett's post hoc test; ***: $p<0.001$ (20)

4.3. Differentially expressed miRNAs identified by microarray profiling

Altogether 1195 miRNAs were analysed by microarray in 4 kidney samples from each group to study differentially expressed miRNAs after LPS administration. One sample was excluded from the EP1.5h group as an outlier based on the Lowess regression analysis. 862 miRNAs were only detected in less than 10% of the samples. From the remaining 333 miRNAs, 71 miRNAs changed significantly in EP and 39 in LP. MiRNAs that changed at least 1.5-fold or 0.75-fold were considered biologically important, and studied further.

Microarray results were analysed by ranking differentially expressed miRNAs based on their fold changes. Only one miRNA was elevated at 1.5 h and 15 miRNAs were upregulated at least 1.5-fold at 6 h (Table 2/A). No miRNA was significantly downregulated with FC below 0.75-fold in the EP groups.

In the LP24h group 6 miRNAs were significantly elevated at least 1.5-fold and 5 were decreased. At 48 h only miR-21a-5p and miR-146a-5p were induced, and 5 miRNAs were suppressed (Table 2/B). Altogether, most miRNAs were differentially regulated at the peak of the inflammatory reaction and renal injury in the EP6h (15 miRNAs) and LP24h groups (11 miRNAs). The miRNome started to get normalized by 48 h.

Table 2. Differentially expressed miRNAs after LPS administration in the microarray analysis. The results are shown as fold changes relative to the control kidneys. FC>1: LPS-induced upregulation, FC<1: reduced expression. (A) Significantly changed miRNAs in EP, (B) significantly changed miRNAs in LP. miRNAs selected for qPCR validation are underlined.miRNAs significantly affected both in EP and LP are highlighted in **bold**. Statistical analysis was performed separately for results in EP (1.5 and 6 h) and LP (24 and 48 h) using one-way ANOVA and Dunnett's post hoc test (double line in the middle separate EP and LP), ns: not significant, *: $p<0.05$, **: $p<0.01$, ***: $p<0.001$. (19)

A. Fold changes in miRNAs differentially expressed in EP				
miRNA	**1.5 h**	**6 h**	**24 h**	**48 h**
miR-204-3p	2.82 ± 0.20 ***	1.88 ± 0.28 ***	1.08 ± 0.10 (ns)	1.21 ± 0.25 (ns)
miR-3102-5p	1.11 ± 0.23 (ns)	2.77 ± 0.52 ***	1.05 ± 0.32 (ns)	1.15 ± 0.25 (ns)
miR-762	1.19 ± 0.27 (ns)	2.69 ± 0.34 ***	1.16 ± 0.32 (ns)	1.24 ± 0.22 (ns)
miR-2137	0.96 ± 0.01 (ns)	2.61 ± 0.26 ***	1.41 ± 0.13 (ns)	1.42 ± 0.63 (ns)
miR-3090-5p	1.21 ± 0.16 (ns)	2.50 ± 0.61 *	1.11 ± 0.35 (ns)	1.36 ± 0.42 (ns)
miR-2861	1.06 ± 0.29 (ns)	2.46 ± 0.40 **	2.22 ± 0.72 **	1.49 ± 0.48 (ns)
miR-665-3p	1.25 ± 0.22 (ns)	2.32 ± 0.22 ***	0.93 ± 0.13 (ns)	0.98 ± 0.11 (ns)
miR-5129-5p	1.17 ± 0.34 (ns)	2.25 ± 0.69 *	0.94 ± 0.37 (ns)	0.95 ± 0.15 (ns)
miR-21a-3p	1.36 ± 0.12 (ns)	2.00 ± 0.20 ***	1.88 ± 0.18 ***	1.34 ± 0.17 (ns)
miR-5116	1.05 ± 0.07 (ns)	1.76 ± 0.17 ***	1.20 ± 0.18 (ns)	1.00 ± 0.15 (ns)
miR-3100-3p	1.03 ± 0.08 (ns)	1.67 ± 0.18 ***	1.28 ± 0.22 (ns)	1.10 ± 0.11 (ns)
miR-711	1.00 ± 0.08 (ns)	1.66 ± 0.24 **	1.23 ± 0.08 (ns)	1.31 ± 0.47 (ns)
miR-466n-3p	1.01 ± 0.06 (ns)	1.61 ± 0.25 *	1.02 ± 0.20 (ns)	0.90 ± 0.08 (ns)
miR-223-3p	1.40 ± 0.20 (ns)	1.60 ± 0.10 **	1.33 ± 0.12 *	1.23 ± 0.16 (ns)
miR-3474	1.01 ± 0.01 (ns)	1.60 ± 0.24 **	1.12 ± 0.09 (ns)	1.02 ± 0.13 (ns)
B. Fold changes in miRNAs differentially expressed in LP				
miRNA	**1.5 h**	**6 h**	**24 h**	**48 h**
miR-21a-5p	1.07 ± 0.2 (ns)	1.39 ± 0.18 *	4.44 ± 0.66 ***	4.59 ± 1.34 **
miR-451a	1.63 ± 0.98 (ns)	1.08 ± 0.33 (ns)	3.76 ± 1.56 **	2.22 ± 2.41 (ns)
miR-144-3p	1.37 ± 0.87 (ns)	1.10 ± 0.24 (ns)	2.56 ± 1.04 **	1.65 ± 1.43 (ns)
miR-2861	1.06 ± 0.29 (ns)	2.46 ± 0.40 **	2.22 ± 0.72 **	1.49 ± 0.48 (ns)
miR-21a-3p	1.36 ± 0.12 (ns)	2.00 ± 0.20 ***	1.88 ± 0.18 ***	1.34 ± 0.17 (ns)
miR-146a-5p	1.10 ± 0.08 (ns)	0.98 ± 0.08 (ns)	1.51 ± 0.14 **	1.58 ± 0.21 **
miR-1839-3p	1.02 ± 0.21 (ns)	0.92 ± 0.24 (ns)	0.57 ± 0.09 **	0.74 ± 0.16 **
miR-34c-3p	0.96 ± 0.19 (ns)	0.87 ± 0.24 (ns)	0.57 ± 0.17 **	0.68 ± 0.16 **
miR-150-5p	1.01 ± 0.20 (ns)	0.79 ± 0.13 (ns)	0.59 ± 0.06 ***	0.63 ± 0.13 ***
miR-129-1-3p	0.90 ± 0.08 (ns)	0.81 ± 0.06 *	0.70 ± 0.05 ***	0.65 ± 0.10 ***
miR-34b-3p	1.01 ± 0.11 (ns)	0.85 ± 0.16 (ns)	0.74 ± 0.04 **	0.81 ± 0.12 (ns)
miR-3070a-5p/ miR-3070b-5p	1.05 ± 0.11 (ns)	0.85 ± 0.09 *	0.78 ± 0.08 (ns)	0.71 ± 0.07 **

4.4. Confirmation of miRNA microarray results

The top four most upregulated miRNAs from each group were validated by qPCR. The changes in miR-762 expression were verified at all time points (Fig. 3/g, h). Changes in expression of miR-204-3p and miR-665 could not be confirmed in EP (Fig. 3/a,b and e,f), while miR-2137 and miR-3102-5p could not be amplified by qPCR in the samples.

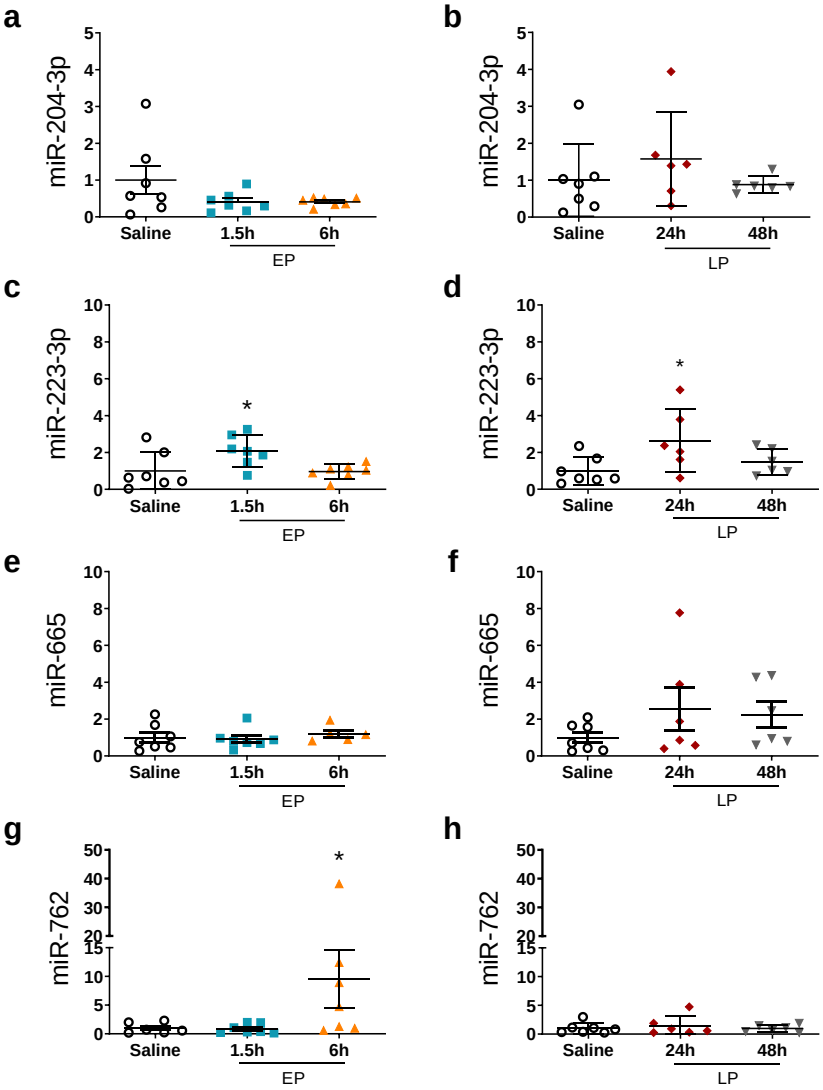

Figure 3. qPCR validation of miRNAs upregulated during the early phase (EP) on the microarray. The relative expression of miRNAs normalized to let-7g-5p (fold changes vs. saline). Left column: EP, right column: LP. (a, b) miR-204-3p; (c, d) miR-

223-3p; (e, f) miR-665; (g, h) miR-762. Data are expressed as mean ± SEM; One-way ANOVA and Dunnett's post hoc test; *: $p<0.05$ (19)

MiR-223-3p was ranked 15th on microarray analysis in EP with significant increases at 6 h (1.6-fold) and 24 h (1.3-fold). The qPCR results demonstrated significant upregulation at 1.5 and 24 h (Fig. 3/c, d).

Upregulation of miR-21a-3p and miR-21a-5p was confirmed by qPCR at most time points (Fig. 4/a-d). Elevated expression of miR-144-3p and miR-451a at 24 h was also verified by qPCR (Fig. 4/g-j). The increased expression of miR-146a-5p was supported by qPCR in LP only at 48 h, and additionally significant upregulation was also detected at 6 h (Fig. 4/e,f).

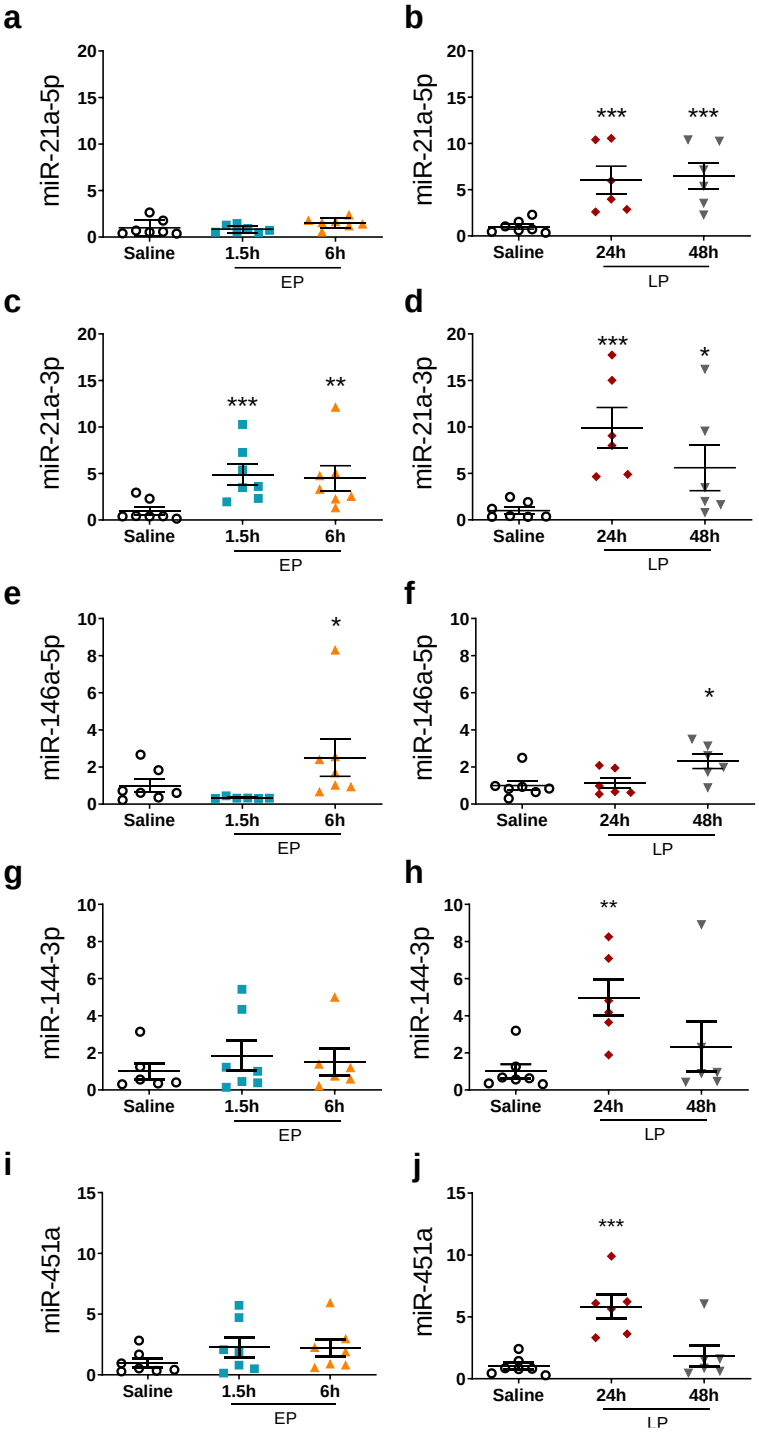

Figure 4. qPCR validation of miRNAs upregulated during the late phase (LP) on microarray. The relative expression of miRNAs was normalized to let-7g-5p (fold changes vs. saline). Left column: EP, right column: LP. (a, b) miR-21a-5p; (c, d) miR-21a-3p; (e, f) miR-146a-5p; (g, h) miR-144a-3p; (i, j) miR-451a. Data are expressed as mean ± SEM; One-way ANOVA and Dunnett's post hoc test; *: $p<0.05$, **: $p<0.01$, ***: $p<0.001$ (19)

Downregulation of miRNAs based on the microarray could not be verified by qPCR (Fig. 5). Expression of miR-34b-3p, miR-129-1-3p and miR-1839-3p was not altered by LPS based on the qPCR quantification. In contrast to microarray results, miR-150-5p and miR-34c-3p were found to be upregulated at 6 and 24 hours, respectively, as measured by qPCR, and were unchanged at the other three time points.

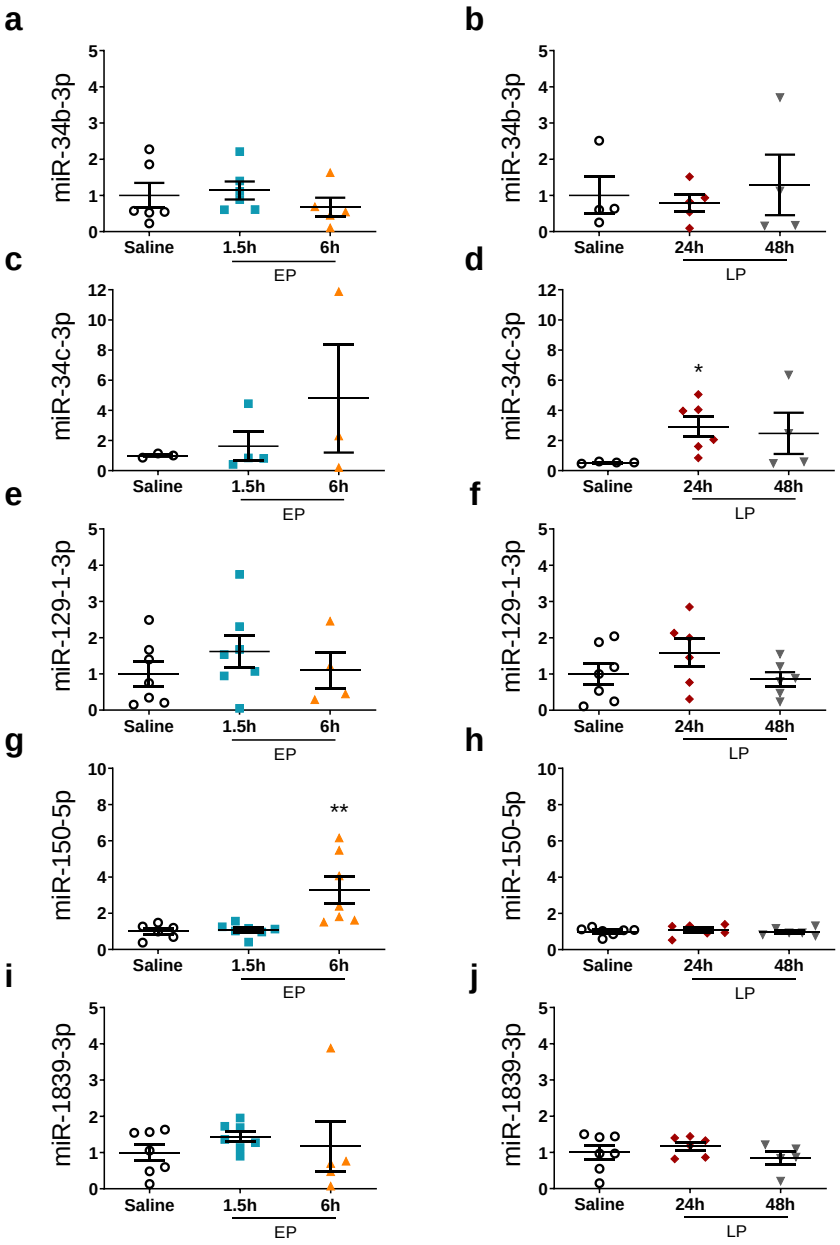

Figure 5. qPCR validation of miRNAs downregulated on microarray. The relative expression of miRNAs normalized to let-7g-5p (fold changes vs. saline). Left column: EP, right column: LP. (a, b) miR-34b-3p; (c, d) miR-34c-3p; (e, f) miR-129-1-3p; (g, h)

miR-150-5p; (i, j) miR-1839-3p. Data are expressed as mean ± SEM; One-way ANOVA and Dunnett's post hoc test; *: p<0.05, **: p<0.01 (19)

4.5. Validated/predicted miRNA targets identified by mass spectrometry

We searched the results of the MS analysis to find differentially expressed proteins that are validated and/or predicted targets of the miRNAs upregulated by LPS. Our MS analysis did not detect any of the so far experimentally validated targets of miR-762 (based on MirTarbase (60)), the miRNA newly associated with septic AKI. However, MS detected 31 proteins in most of the samples from the 732 predicted targets of miR-762 in the miRDB database. One of these proteins, the secretion associated Ras related GTPase 1B (Sar1b) or GTP-binding protein Sar1b seemed to be a relevant association with miR-762, as it's concentration was significantly suppressed 6 h after LPS administration, at the time of the peak upregulation of miR-762 (Fig. 6).

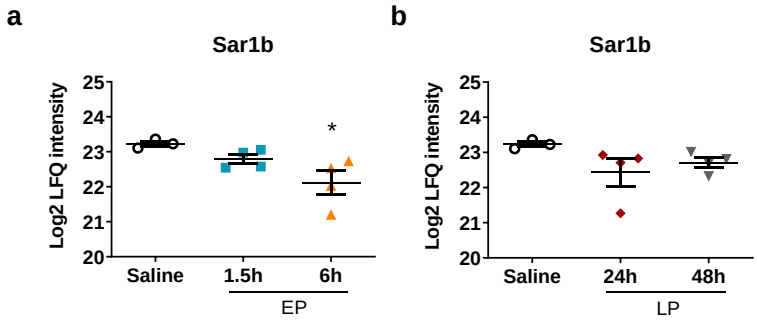

Figure 6. Protein expression of a miR-762 predicted target, secretion associated Ras related GTPase 1B (Sar1b) or GTP-binding protein Sar1b in the kidneys of mice after LPS administration. Log2 transformed label-free quantification (LFQ) intensity values of Sar1b was measured by HPLC-MS/MS. (a) EP, (b) LP. Data are expressed as mean ± SEM; One-way ANOVA and Dunnett's post hoc test; *: p<0.05

We identified a seemingly strong association between miR-144-3p and one of its validated targets, aquaporin-1 (Aqp1). The HPLC-MS/MS analysis detected that Aqp1 protein concentration significantly increased in the kidney in EP and decreased at 24 h (Fig. 7). Aqp1 concentration changed inversely with miR-144-3p at 24 h after treatment with LPS as miR-144-3p was upregulated (Fig. 4/g,h) while Aqp1 was downregulated.

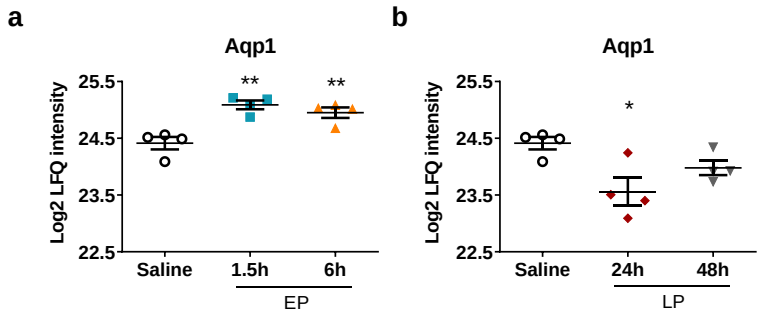

Figure 7. Protein expression of an experimentally validated target of miRNA-144-3p, aquaporin-1 (Aqp1) in mouse kidneys after LPS administration. Log2 transformed label-free quantification (LFQ) intensity values of Aqp1 as determined by HPLC-MS/MS. (a) EP, (b) LP. Data are expressed as mean ± SEM; One-way ANOVA and Dunnett's post hoc test; *: $p<0.05$, **: $p<0.01$. (19)

Furthermore, the MS analysis revealed a few other differentially regulated transporter proteins, which are validated or predicted targets of differentially expressed miRNAs (based on miRDB and/or microRNA.org) that were verified by qPCR in our study.

Solute carrier family 4 member 4 (Slc4a4) (also called the electrogenic sodium bicarbonate cotransporter 1 (NBCe1)) is a predicted target of miR-144-3p and miR-223-3p. Slc4a4 protein concentration was significantly suppressed both at 24 and 48 h (Fig. 8/a, b), while treatment with LPS upregulated both miR-223-3p (Fig. 3/c, d) and miR-144-3p (Fig. 4/g, h) at 24 h.

Another predicted target of miR-144-3p, solute carrier family 22 member 8 (Slc22a8) (also called organic anion transporter 3, Oat3) showed a slow tendency to decrease after LPS administration that became significant at 48 h (Fig. 8/c, d). In parallel, expression of miR-144-3p was significantly upregulated 24 h after LPS administration but was slightly increased at other time points too (Fig. 4/g, h).

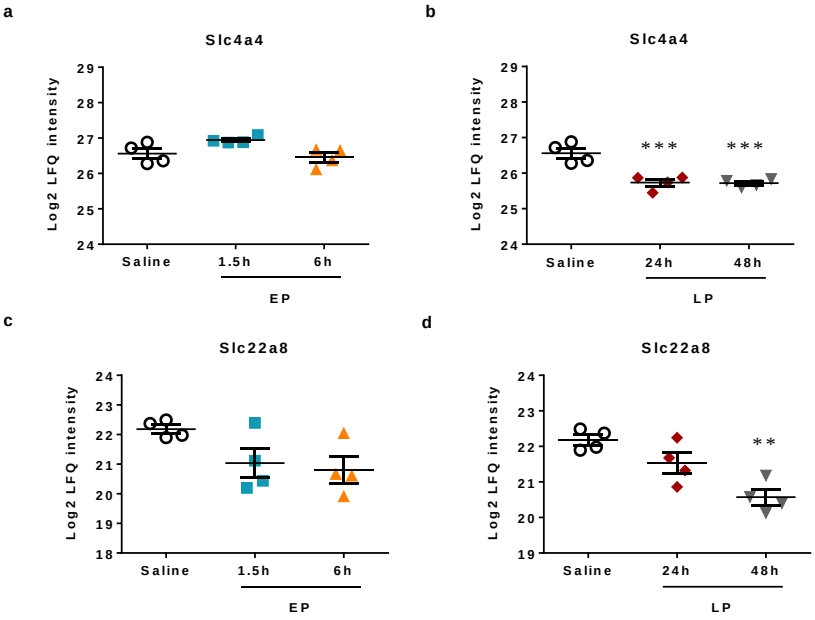

Figure 8. Protein expression of transporters that are predicted miRNA targets in mouse kidneys after LPS administration. Log2 transformed label-free quantification (LFQ) intensity values of proteins were measured by HPLC-MS/MS. Left column (a, c): EP, right column (b, d): LP. (a, b) Slc4a4; (c, d) Slc22a8. Data are expressed as mean ± SEM; One-way ANOVA and Dunnett's post hoc test; **: $p<0.01$, ***: $p<0.001$. (19)

4.6. Acute-phase proteins were the most upregulated proteins in the kidney in the late phase after LPS administration

The analysis of the renal proteome revealed that the changes in protein concentrations were smaller in the EP groups than in the LP groups in response to LPS administration. At 1.5 and 6 h after LPS administration only 10-10 proteins were upregulated at least 4-fold ($log_2FC=2$) (Fig. 9/a, b and Table 3). Proteome changes were the most significant and abundant at 24 h (Fig. 9/c). At 24 h forty-seven, while at 48 h forty-four proteins were upregulated at least 4-fold ($log_2FC=2$) (Table 4). Expression of several proteins was elevated both in EP and LP.

APPs were abundantly present among the most upregulated proteins in LP (Fig. 9/c, d and Table 4). In EP, the established marker of AKI, Lcn-2 was the only APP increased more than 4-fold. However, at 24 h 47% and at 48 h 39% were APPs among the proteins that increased at least 4-fold (Table 4, bold highlight). In LP Lcn-2 was again one of the most strongly induced APPs, as it was the first and second most upregulated protein at 24

and 48 h after LPS administration. Other APPs leading the lists were complement C3 and the 3 chains of fibrinogen, followed by transport proteins (e.g. haptoglobin, hemopexin, ceruloplasmin, transferrin, ferritin heavy chain), protease inhibitors (alpha-2-macroglobulin, inter alpha-trypsin inhibitors), serine protease inhibitors (serpins) and amyloids.

Table 3. Proteins significantly upregulated at least 4-fold ($log_2FC=2$) relative to those in kidneys of saline-injected control mice in EP. APPs are highlighted in bold. log_2FC: log2 transformed values of fold change. (20)

	EP1.5h	**log_2FC**	**EP6h**	**log_2FC**
1	GTPase HRas	4.36	GTPase HRas	4.75
2	Chitinase-like protein 3	3.60	Chitinase-like protein 3	4.66
3	Protein S100-A9	2.59	**Lipocalin-2**	3.55
4	Succinate-semialdehyde dehydrogenase, mitochondrial	2.30	H-2 class I histocompatibility antigen, L-D alpha chain	3.31
5	Mesencephalic astrocyte-derived neurotrophic factor	2.29	CD151 antigen	3.28
6	CD151 antigen	2.27	Protein S100-A9	3.12
7	S-adenosylmethionine synthase isoform type-2	2.26	Major urinary protein 3	2.78
8	Proteasome subunit alpha type-7	2.20	Transmembrane emp24 domain-containing protein 2	2.36
9	Peptidyl-prolyl cis-trans isomerase FKBP3	2.13	Proteasome subunit alpha type-7	2.20
10	Transmembrane emp24 domain-containing protein 2	2.10	Cytochrome c oxidase subunit 7C, mitochondrial	2.04

Table 4. List of proteins significantly upregulated at least 4-fold ($log_2FC=2$) relative to those in control kidneys of mice in LP. APPs are highlighted in bold. log_2FC: log2 transformed values of fold change. (20)

	LP24h	**log_2FC**	**LP48h**	**log_2FC**
1	**Lipocalin-2**	6.36	H-2 class I histocompatibility antigen, L-D alpha chain	6.03
2	**Complement C3**	6.09	**Lipocalin-2**	5.71
3	**Hemopexin**	5.90	**Hemopexin**	5.62
4	**Fibrinogen alpha chain**	5.85	**Complement C3**	5.58
5	H-2 class I histocompatibility antigen, L-D alpha chain	5.69	Interferon-inducible GTPase 1	5.19
6	**Fibrinogen gamma chain**	5.67	**Fibrinogen gamma chain**	5.12
7	**Fibrinogen beta chain**	5.62	**Haptoglobin**	5.01
8	Interferon-inducible GTPase 1	5.59	Interferon-induced guanylate-binding protein 2	4.86
9	Interferon-induced guanylate-binding protein 2	5.57	**Fibrinogen alpha chain**	4.76
10	**Haptoglobin**	5.25	**Fibrinogen beta chain**	4.75
11	T cell specific GTPase 1	5.21	Immunity-related GTPase family M protein 1	4.14
12	**Inter alpha-trypsin inhibitor, heavy chain 4**	4.83	**Serum amyloid A-2 protein**	3.54
13	Immunity-related GTPase family M protein 1	4.66	Major vault protein	3.52
14	**Serine protease inhibitor A3K**	4.49	Chitinase-like protein 3	3.46
15	**Alpha-2-macroglobulin**	4.21	**Beta-2-microglobulin**	3.45
16	Chitinase-like protein 3	3.96	**Serine protease inhibitor A3K**	3.44
17	**Serum amyloid A-2 protein**	3.92	T cell specific GTPase 1	3.28
18	CD151 antigen	3.82	**Alpha-1-acid glycoprotein 1, Alpha-1-acid glycoprotein 2**	3.24
19	**Ceruloplasmin**	3.72	Napsin-A	3.21
20	Major vault protein	3.72	**Inter alpha-trypsin inhibitor, heavy chain 4**	3.19

	LP24h	log_2FC	LP48h	log_2FC
21	Interferon-induced transmembrane protein 3	3.45	**Ceruloplasmin**	3.07
22	Murinoglobulin-1, Murinoglobulin-2	3.45	**Alpha-2-macroglobulin**	3.03
23	Major urinary protein 3	3.36	**Serum amyloid A-1 protein**	3.00
24	Proteasome activator complex subunit 2	3.11	Interferon-induced transmembrane protein 3	2.91
25	**Alpha-1-antitrypsin 1-3, Alpha-1-antitrypsin 1-1**	3.00	Cytochrome P450 4A10	2.83
26	Guanylate-binding protein 4	3.00	Proteasome activator complex subunit 2	2.82
27	**Beta-2-microglobulin**	2.90	**Ferritin heavy chain**	2.69
28	**Ferritin heavy chain**	2.79	Guanylate-binding protein 4	2.57
29	**Serine protease inhibitor A3N**	2.74	Xanthine dehydrogenase/oxidase	2.55
30	Deoxynucleoside triphosphate triphosphohydrolase SAMHD1	2.62	H-2 class II histocompatibility antigen, A-Q beta and A-D beta chain	2.50
31	Kininogen-1	2.61	Deoxynucleoside triphosphate triphosphohydrolase SAMHD1	2.45
32	Proteasome activator complex subunit 1	2.52	Proteasome activator complex subunit 1	2.43
33	Proteasome subunit alpha type-7	2.48	[Pyruvate dehydrogenase (acetyl-transferring)] kinase isozyme 4, mitochondrial	2.42
34	[Pyruvate dehydrogenase (acetyl-transferring)] kinase isozyme 4, mitochondrial	2.45	Proteasome subunit alpha type-7	2.40
35	Glucose 1-dehydrogenase, 6-phosphogluconolactonase	2.41	Long-chain-fatty-acid--CoA ligase 4	2.36
36	Inorganic pyrophosphatase	2.39	**von Willebrand factor A domain-containing protein 5A**	2.33
37	Signal transducer and activator of transcription 1	2.30	Prelamin-A/C; Lamin-A/C	2.30
38	**Apolipoprotein E**	2.28	Basal cell adhesion molecule	2.29

	LP24h	log_2FC	LP48h	log_2FC
39	**Serotransferrin**	2.26	Glucose 1-dehydrogenase, 6-phosphogluconolactonase	2.27
40	**Serum amyloid A-1 protein**	2.25	Adenosine kinase	2.27
41	Protein S100-A9	2.25	H-2 class I histocompatibility antigen K-W28 alpha and K-Q alpha chain	2.21
42	**Vitamin D-binding protein**	2.24	Signal transducer and activator of transcription 1	2.21
43	Actin-related protein 2/3 complex subunit 2	2.23	Microsomal glutathione S-transferase 1	2.12
44	**Serum albumin**	2.22	Macrophage-capping protein	2.00
45	High mobility group protein B2	2.16		
46	**Apolipoprotein A-I**	2.14		
47	ADP-ribosylation factor 4	2.08		

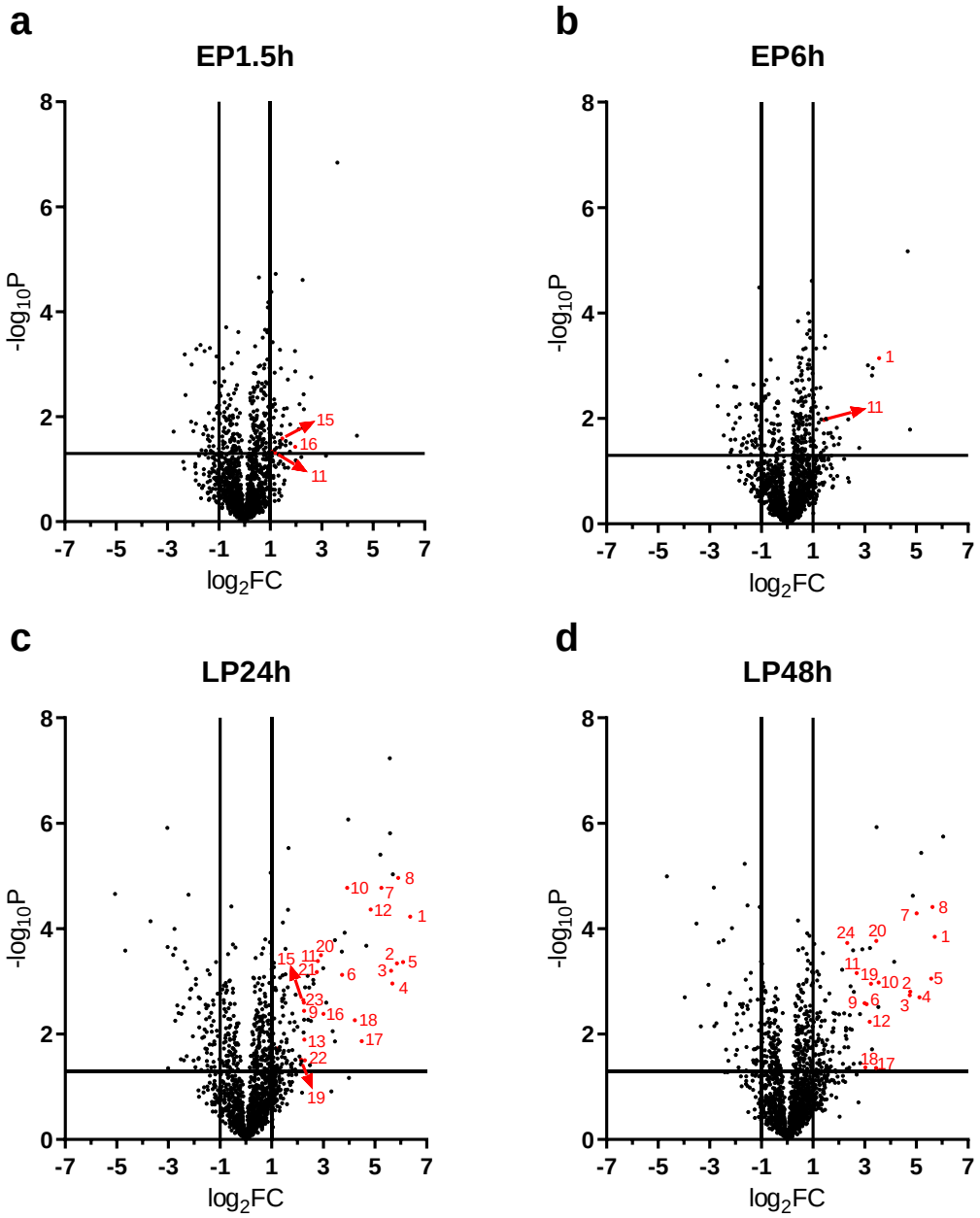

Figure 9. Changes in renal protein expression after LPS administration. P values (given as $-\log_{10}$p values) are plotted as a function of fold changes (given as $\log_2$FC). Vertical lines indicate a 2-fold change, and horizontal lines indicate a significance level of *P*=0.05. APPs are marked with red dots (1: Lcn-2, 2: fibrinogen-α, 3: fibrinogen-β, 4: fibrinogen-γ, 5: complement C3, 6: ceruloplasmin, 7: haptoglobin, 8: hemopexin, 9: serum amyloid A-1, 10: serum amyloid A-2, 11: ferritin heavy chain, 12: inter alpha-trypsin inhibitor, heavy chain 4, 13: transferrin, 14: serum albumin, 15: alpha-1-antitrypsin 1-3 and 1-1, 16: serine protease inhibitor A3K, 17: alpha-2-macroglobulin,

18: apolipoprotein A1, 19: alpha-1-acid glycoprotein, 20: beta-2-microglobulin, 21: serine protease inhibitor A3N, 22: apolipoprotein E, 23: vitamin D-binding protein, 24: von Willebrand factor A domain-containing protein 5A). (a) 1.5 h, (b) 6 h, (c) 24 h, (d) 48 h. (20)

Since APPs were at the top of the lists of upregulated proteins in such a high proportion in LP, we collected all the significantly upregulated APPs in Table 5. A number of APPs were increased in the kidneys after LPS administration at both 24 and 48 h: fibrinogen-α, -β, -γ, complement C3, inter alpha-trypsin inhibitor heavy chain 4, transferrin, haptoglobin, hemopexin, two isoforms of serum amyloid A (Saa1 and Saa2), ceruloplasmin, alpha-2-macroglobulin (A2m), serine protease inhibitor A3K (Serpina3k) and beta-2-microglobulin (B2m). Serine protease inhibitor A3N (Serpina3n), apolipoproteins A1 (ApoA1) and E (ApoE), vitamin D-binding protein or Gc-globulin (DBP) and inter-alpha-trypsin inhibitor heavy chain H1 (Itih1) were significantly increased only at 24 h. Von Willebrand factor A domain-containing protein 5A (Vwa5a) and alpha-1-acid glycoprotein (A1AGP) were upregulated after LPS administration only at 48 h.

Renal protein concentration of ferritin heavy chain was significantly increased at all 4 time points. Alpha-1-antitrypsin (Serpina1) protein was significantly elevated at 1.5, 24 and 48 h. Albumin concentration was significantly elevated at 1.5 and 24 h, while it was at control level at 6 and 48 h.

Table 5. Log2 transformed label-free quantification (LFQ) intensity values of APPs measured using MS in the kidneys of mice after LPS administration. Values shown are mean±SD. *: $p<0.05$, **: $p\leq0.01$, ***: $p\leq0.001$. Statistical analysis of data in EP (1.5 and 6 h) and LP (24 and 48 h) was done separately (marked by a middle double line). Lcn-2: lipocalin-2, C3: complement C3, Fga: fibrinogen-α, Fgb: fibrinogen-β, Fgg: fibrinogen-γ, Saa: serum amyloid A, Cp: ceruloplasmin, Hp: haptoglobin, Hpx: hemopexin, Itih4: inter alpha-trypsin inhibitor heavy chain 4, FHC: ferritin heavy chain, Tf: transferrin, Alb: serum albumin, Serpina1: alpha-1-antitrypsin, Serpina3k: serine protease inhibitor A3K, Serpina3n: serine protease inhibitor A3N, A2m: alpha-2-macroglobulin, B2m: beta-2-microglobulin, ApoA1: apolipoprotein A1, ApoE: apolipoprotein E, A1AGP: α-1-acid glycoprotein, Itih1: inter alpha-trypsin inhibitor

heavy chain 1, DBP: vitamin D-binding protein, Vwa5a: von Willebrand factor A domain-containing protein 5A. (20)

	saline	**EP1.5h**	**EP6h**	**LP24h**	**LP48h**
Lcn-2	20.65 ± 1.10	20.31 ± 1.00	*** 24.20 ± 0.23	*** 27.01 ± 0.66	*** 26.36 ± 0.77
C3	21.94 ± 1.69	23.29 ± 1.23	21.24 ± 1.20	*** 28.03 ± 0.41	*** 27.51 ± 0.69
Fga	21.78 ± 1.61	23.20 ± 2.08	22.85 ± 1.77	*** 27.63 ± 0.53	*** 26.54 ± 0.67
Fgb	21.53 ± 1.56	21.84 ± 0.85	21.36 ± 0.55	*** 27.15 ± 0.74	*** 26.28 ± 0.88
Fgg	21.26 ± 1.89	22.06 ± 1.42	23.00 ± 1.58	*** 26.93 ± 0.44	*** 26.38 ± 0.55
Saa1	20.84 ± 0.79	21.03 ± 0.79	21.01 ± 0.59	** 23.09 ± 0.57	*** 23.84 ± 0.92
Saa2	20.38 ± 0.50	19.77 ± 0.78	21.28 ± 0.34	*** 24.30 ± 0.39	*** 23.91 ± 1.09
Cp	21.34 ± 1.15	20.52 ± 0.68	19.85 ± 0.79	*** 25.06 ± 0.29	*** 24.41 ± 0.50
Hp	21.06 ± 0.62	20.53 ± 0.48	21.04 ± 1.10	*** 26.31 ± 0.58	*** 26.07 ± 0.76
Hpx	22.15 ± 0.84	20.66 ± 0.37	21.91 ± 1.03	*** 28.05 ± 0.27	*** 27.77 ± 0.67
Itih4	20.77 ± 0.76	20.73 ± 0.92	21.14 ± 0.49	*** 25.60 ± 0.51	** 23.96 ± 1.33
FHC	23.57 ± 0.72	* 24.65 ± 0.47	** 24.99 ± 0.28	*** 26.36 ± 0.32	*** 26.26 ± 0.43
Tf	26.25 ± 1.26	27.36 ± 0.44	26.83 ± 0.46	** 28.51 ± 0.27	* 27.79 ± 0.47
Alb	29.60 ± 0.85	* 31.06 ± 0.51	29.97 ± 0.29	*** 31.82 ± 0.20	30.47 ± 0.50
Serpina1a,c	23.84 ± 1.30	* 25.81 ± 0.70	25.44 ± 0.37	*** 26.84 ± 0.28	* 25.32 ± 0.34
Serpina3k	22.88 ± 2.55	26.04 ± 0.79	25.22 ± 0.96	** 27.37 ± 0.52	* 26.32 ± 0.91
Serpina3n	20.53 ± 0.75	20.83 ± 0.84	20.90 ± 0.47	** 23.27 ± 0.41	22.06 ± 1.18
A2m	22.13 ± 1.92	23.45 ± 2.12	21.00 ± 0.52	** 26.34 ± 0.52	* 25.16 ± 1.37
B2m	20.80 ± 0.75	20.05 ± 0.49	21.82 ± 1.45	*** 23.70 ± 0.24	*** 24.25 ± 0.37
ApoA1	25.16 ± 1.35	26.48 ± 0.67	25.26 ± 0.34	* 27.30 ± 0.68	26.22 ± 0.35
ApoE	20.42 ± 1.10	21.58 ± 1.12	20.58 ± 0.95	* 22.70 ± 1.20	21.46 ± 0.81

	saline	EP1.5h	EP6h	LP24h	LP48h
A1AGP	20.12 ± 0.96	20.25 ± 0.58	20.57 ± 0.56	21.12 ± 1.02	*** 23.36 ± 0.55
Itih1	20.10 ± 0.68	21.14 ± 0.50	21.08 ± 1.02	* 21.32 ± 0.36	21.10 ± 0.69
DBP	20.54 ± 0.75	21.04 ± 0.45	20.46 ± 0.29	*** 22.78 ± 0.50	21.33 ± 0.37
Vwa5a	20.75 ± 0.56	20.56 ± 0.58	20.44 ± 0.69	22.29 ± 1.57	* 23.08 ± 0.12

4.7. Acute-phase protein synthesis was stimulated in the kidney after LPS

We performed qPCR analysis to verify that the source of upregulated APPs was the kidney. We found that LPS significantly upregulated the renal mRNA expression of several APPs (Fig. 10). Gene expression of ceruloplasmin and haptoglobin was induced already at 1.5 h. Expression of complement C3, fibrinogen-α, -β, -γ, serum amyloid A, ceruloplasmin, haptoglobin, hemopexin, inter alpha-trypsin inhibitor heavy chain 4, and ferritin heavy chain was upregulated by LPS at 6, 24 and 48 h. Transferrin expression was upregulated in the kidneys only in LP.

The mRNA expression of fibrinogen-α, -β, -γ, serum amyloid A, ceruloplasmin, hemopexin and ferritin heavy chain started to decrease at 48 h. Expression of complement C3 and transferrin also showed a decreasing tendency at 48 h, though the difference was not statistically significant.

Albumin mRNA expression was unchanged in the kidneys during EP but started to decrease at 24 h and was significantly downregulated at 48 h.

The two isoforms of alpha-1-antitrypsin (Serpina1a and Serpina1c) were not differentiated by MS. To overcome this limitation, we measured their mRNA expression separately, but we could not amplify either isoform, suggesting that their renal expression was below detection limit. However, using the primers designed by Zager et al. (64) we found that alpha-1-antitrypsin mRNA was downregulated in the kidneys in all LPS-treated groups. As the 1d isoform is also amplified by this primer pair besides the 1a and 1c isoforms, the decreased mRNA expression could be attributed to Serpina1d that was not detected by MS. Expression of the serine protease inhibitor A3K mRNA was also below detection limit in all kidney samples.

Expression of another inflammatory marker, chitinase-like protein 3 (Chil3) was enhanced at 6 and 24 h after LPS administration and was still upregulated at 48 h, but to a lesser extent.

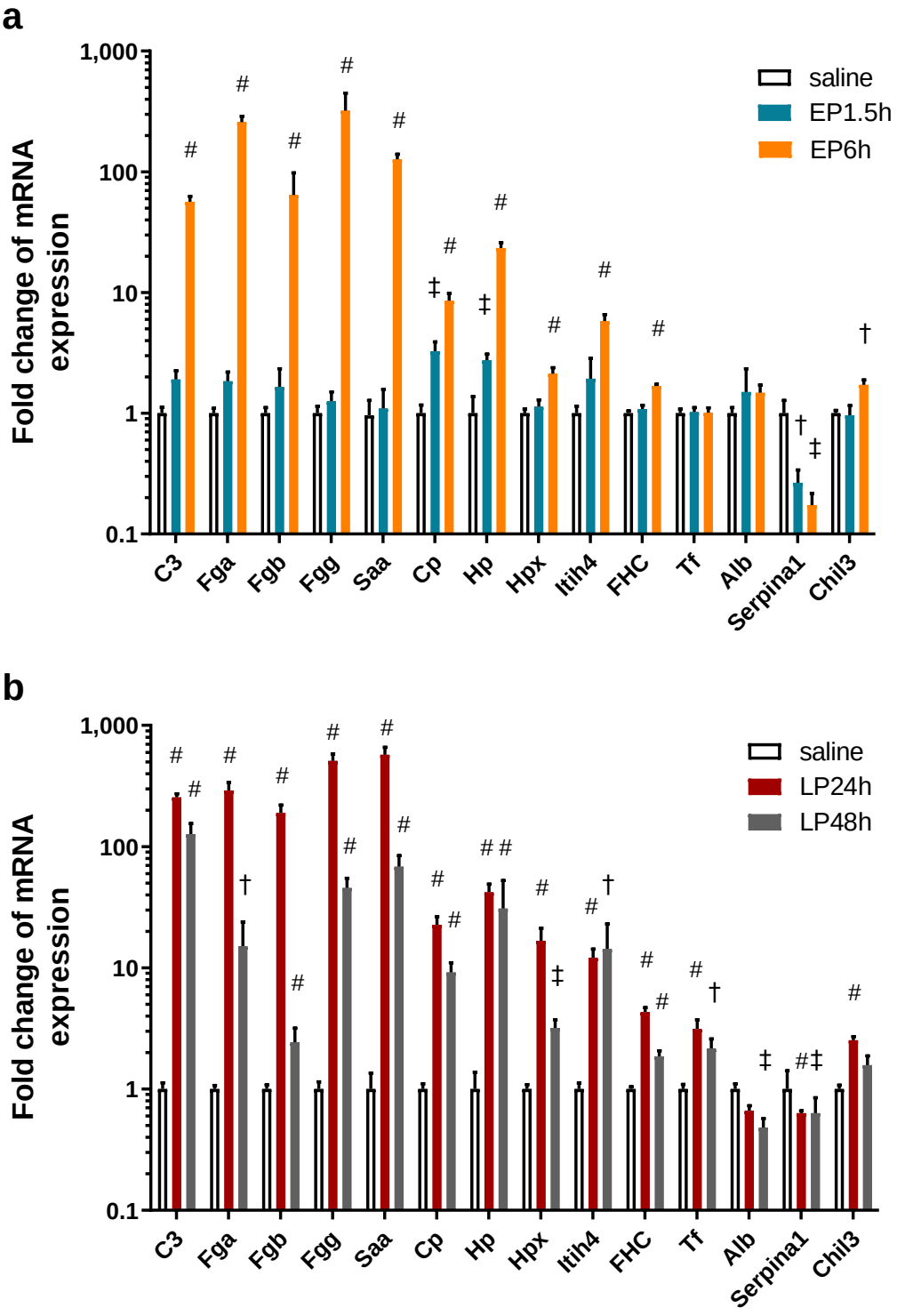

Figure 10. Fold changes of mRNA expression of APPs relative to the respective control kidneys after LPS administration in mice. Data are expressed as mean ± SEM;

One-way ANOVA and Dunnett's post hoc test; †: $p<0.05$, ‡: $p\leq0.01$, #: $p\leq0.001$. C3: complement C3, Fga: fibrinogen-α, Fgb: fibrinogen-β, Fgg: fibrinogen-γ, Saa: serum amyloid A, Cp: ceruloplasmin, Hp: haptoglobin, Hpx: hemopexin, Itih4: inter alpha-trypsin inhibitor heavy chain 4, FHC: ferritin heavy chain, Tf: transferrin, Alb: serum albumin, Serpina1: alpha-1-antitrypsin, Chil3: chitinase-like protein 3. (a) 1.5 h, 6 h. (b) 24 h, 48 h. (20)

5. Discussion

LPS induced AKI, as demonstrated by the elevated plasma urea concentrations and the upregulated renal mRNA expression of Tnf-α, IL-6 and Lcn-2. Protein expression of Lcn-2, a marker of kidney injury was enhanced too. Several factors including plasma urea concentration and mRNA expression of IL-6 and Lcn-2 started to decrease at 48 h after endotoxin administration, indicating the onset of recovery.

The renal miRNome responded to LPS administration mainly by upregulation of miRNAs. This is the first study that addressed the time-dependent changes in the miRNome in LPS-induced AKI using multiplex methods. Although severe impairment of the renal function was observed already at 1.5 h, very few miRNAs were upregulated at this early time point. The most robust miRNA responses were detected at 6 and 24 h. In LP the expression of miR-21a-duplex, miR-144-3p/451a, miR-146a-5p and miR-223-3p was elevated at 24 and/or 48 h. The decline of AKI markers at 48 h indicated a recovery that was associated with normalized expression of several miRNAs.

In most cases, changes in the expression of miRNAs in the microarray were successfully confirmed by qPCR. However, validation of the microarray results by qPCR revealed some false positive hits. Based on the qPCR measurements renal expression of miR-34b-3p and miR-1839-3p (downregulated on the array), furthermore miR-204-3p and miR-665 (upregulated on the array) was not altered by LPS. In addition, miR-34c-3p was detected by qPCR to be significantly increased as opposed to the downregulation observed in the miRNA microarray. Finally, miR-2137 and 3102-5p could not be amplified by qPCR. It is well-known that some results obtained by multiplex techniques (e.g. microarrays) can be misleading (66,67). There are many potential reasons for this problem, such as a multitude of investigated genes, small sample size and polymorphisms in the target and the probe sequence (68–70). Our study also supports the necessity to validate array data by other techniques such as qPCR. Only those miRNAs are discussed that were verified by qPCR after being detected as differentially expressed by the miRNA microarray.

To find potential molecular and/or pathophysiological pathways that could be influenced by the observed miRNome changes, we searched for relevant miRNA-protein associations. We searched our proteomic data obtained by MS analysis for validated and

predicted protein targets of the differentially expressed miRNAs. We focused on target proteins that were expressed in opposite direction to their target miRNAs.

A novel finding in our study is that miR-762 was the most upregulated among the miRNAs at 6 h, at the time of the peak miRNome response in EP. MiR-762 was indicated to play a role in remote ischemic preconditioning in mouse CD34+ bone marrow cells (71). Our results newly indicate a potential role of miR-762 in LPS-induced AKI, and possibly in the endotoxin-mediated preconditioning of the kidney (13). We found that the predicted target of miR-762, the secretion associated Ras related GTPase 1B (Sar1b) is likely to be regulated by miR-762 also in our study. Sar1b belongs to the Sar1-ADP ribosylation factor family of small GTPases (72) that regulate the intracellular trafficking of proteins in protein-coated vesicles. Sar1b was shown to have a function in inflammation and oxidative stress (73). Along with miR-762, we newly identified that Sar1b could possibly play a role in septic AKI. Other previously described targets of miR-762, such as TLRs and interferon regulatory factors (74) were not detected by MS in our study, most likely due to the limitations of the total proteome analysis.

Expression changes of the closely clustered and evolutionally conserved bicistronic miRNAs, miR-144 and miR-451 (75,76) moved together. MiR-144-3p was demonstrated to play a protective role in remote preconditioning of the heart (induced by limb ischemia) (77). MiR-451a was found to be upregulated after LPS administration in RAW267.4 cells (78). However, the role of the miR-144/451 cluster in the LPS-induced AKI has not been studied previously.

The total proteome analysis revealed that the renal protein concentration of apuaporin-1 (Aqp1) decreased at 24 h. Aqp1 is an already validated target of miR-144-3p (79). Inverse regulation of miR-144-3p and Aqp1 at 24 h suggested that Aqp1 was possibly suppressed by miR-144-3p. Both mRNA and protein expression of Aqp1 was demonstrated in previous studies to be downregulated by LPS in mouse kidneys (80,81). Similarly to our results, literature data show that renal protein concentration of Aqp1 first increased and later decreased (82). Renal ischemia-reperfusion injury suppressed the mRNA expression of Aqp1 too (83). Also, urinary exosomal release of aquaporins AQP1 and AQP2 was decreased in ischemic AKI (84). Furthermore, endotoxin administration induced a more severe kidney injury in Aqp1 knockout mice (85), while overexpression of Aqp1 was protective in LPS-treated HK-2 cells (86).

Solute carrier family 22 member 8 (Slc22a8), also termed as organic anion transporter 3 (Oat3), is another predicted target of miR-144-3p. Our results indicated that Slc22a8 (Oat3) was downregulated and thus could be inversely regulated by miR-144-3p too. Both sepsis and ischemia impair renal tubular function, including anion excretion (87). LPS was previously demonstrated to significantly downregulate the expression of Slc22a8 (Oat3) (88) time and dose dependently (87).

Our results strongly support an important role for miR-21 duplex in septic AKI, as miR-21a-5p was one of the most upregulated miRNAs, while miR-21a-3p was also induced by LPS at all time points. MiR-21 was already described to modulate renal injury caused by LPS (49). As opposed to the 3p arm, miR-21a-5p was only upregulated at later time points. In a previous study we also found that miR-21a induction was a late event as it was first elevated 24 hours after an ischemic renal injury (89). The immune-regulatory roles of miR-21 are well characterized (90,91), and that was also supported by our study.

MiR-146a-5p was already reported to play a role in septic AKI (52). Our results are in agreement with this finding. MiR-146a-5p was also described to regulate the pro-inflammatory cytokine production in LPS-stimulated macrophages, and may also suppress the monocytic immune response (92). In addition, miR-146a-5p mediated the endotoxin-induced cross-tolerance to renal ischemia through the activation of NF-κB signalling (93).

Expression of miR-223-3p was significantly elevated at 1.5 and 24 h after LPS. MiR-223 has a role in haematopoiesis (94), and it has been associated with inflammatory conditions such as sepsis (95) and liver ischemia (96). Wang et al. (97) reported that the inflammatory response to LPS was downregulated by miR-223 in RAW 264.7 murine macrophages through the suppression of the NF-κB signalling pathway. In sepsis its role seems controversial because LPS-induced AKI (a sterile model of septic AKI) was exaggerated, while polymicrobial infection-induced AKI was attenuated in miR-223 knock-out (KO) mice (51). MiR-223 may not only have model-specific but also organ-specific functions, as polymicrobial infection aggravated myocardial dysfunction and mortality in miR-223 KO mice (98). Our results are also in favour of the role for miR-223-3p in LPS-induced AKI.

During the target search, the electrogenic sodium bicarbonate cotransporter 1 (Slc4a4 or NBCe1) was found to be inversely regulated to both miR-144-3p and miR-

223-3p. Thus, it is possible that miR-144 and miR-223 downregulated Slc4a4 after LPS in LP. In support of this finding, miR-223-3p was described to downregulate SLC4A4 in clear cell renal cell carcinoma, thereby promoting cell proliferation and metastasis (99). Slc4a4 might be associated with septic conditions based on our results.

Further analysis of the overall renal proteome changes revealed that APPs were abundantly present among the most upregulated proteins in LP.

APP secretion is a well-known consequence of inflammatory stimuli including LPS or sepsis. Although the common view is that the major source of plasma APPs is the liver (23,100), it has been demonstrated that several APPs are also expressed in other organs even under physiological conditions. For example, ferritin is produced in all organs including the kidneys (101). Furthermore, haptoglobin is expressed in the lung and skin (23), hemopexin in the retina and nervous system (102), ceruloplasmin in the mammary gland, kidney and brain (103), transferrin in the brain (104), complement C3 in the kidney and immune cells (105), and serum amyloid A in many tissues including the kidney (106). APPs are expressed physiologically in extrahepatic tissues only at a low level, but local injuries can increase their extrahepatic production too (23).

Although some APPs have already been demonstrated to be also produced in the kidney, our comprehensive description of a massive, combined renal APR in sepsis is a novelty. Our results are in line with previous isolated findings showing that LPS induced renal mRNA and/or protein expression of all three chains of fibrinogen (34), complement C3 (40,41), haptoglobin (36–38), hemopexin (39), ceruloplasmin (35) and serum amyloid A (35,36) 24 hours after its administration, while it downregulated the expression of albumin (43). We identified further APPs that were upregulated by LPS in the kidney such as inter alpha-trypsin inhibitor heavy chain 4, ferritin heavy chain, transferrin, apolipoprotein A1 and E, vitamin D-binding protein, alpha-2-macroglobulin, serine protease inhibitors A3K and A3N, inter-alpha-trypsin inhibitor heavy chain H1, and alpha-1-antitrypsin. Unlike in humans, transferrin is known as a positive APP in mice (107).

Expression of chitinase-like protein 3 (Chil3) was also induced by LPS in the kidney. It belongs to the chitinase-like protein family in rodents. It is a chemoattractant for eosinophils and a marker of murine N2 neutrophils and M2 macrophages (108–111). Chitinase-3-like protein 1 (CHI3L1), a highly homologous member of the chitinase-like

protein family, is regarded as an APP in humans (112). Elevated serum concentrations of both CHI3L1 and Chil3 were detected in septic mice (113), suggesting a possible role for Chil3 in the APR too.

The LPS-induced renal APR probably has a homeostatic function in tissue protection (22). APPs can contribute to this in many ways. First of all, some effectors of the immune system like complement C3 belong to this group of proteins (114). Many APPs have antioxidant or anti-inflammatory activity (e.g. haptoglobin (115), hemopexin (116), ceruloplasmin (117), inter alpha-trypsin inhibitor heavy chain 4 (118), apolipoproteins (119,120) and alpha-1-acid glycoprotein (121)) and/or cytoprotective scavenger functions (e.g. haptoglobin sequesters haemoglobin (115), hemopexin binds to heme and bivalent metal ions (116), ferritin heavy chain (122) and transferrin (123) have affinity for free Fe, while vitamin D-binding protein (124) and apolipoprotein A1 (119) neutralize LPS). Some APPs attract immune cells (e.g. serum amyloid A (125), fibrinogen (126) and chitinase-like protein 3 (108)), some protect tissues from proteolytic damage (e.g. alpha-2-macroglobulin (127) and alpha-1 antitrypsin (128)), while others facilitate tissue repair (e.g. fibrinogen (114)).

Enhancing cell survival is another possible role of APPs produced locally in the kidney (7). For example, ferritin heavy chain (129) and the heme-hemopexin complex (116) were described to inhibit apoptosis. The function of ferritin heavy chain in AKI has already been studied. Proximal tubule-specific ferritin heavy chain knockout mice had worse outcomes in unilateral ureteral obstruction, cisplatin-induced AKI or rhabdomyolysis than wild type mice (130,131). Furthermore, renal overexpression of ferritin heavy chain prior to ischemia-reperfusion injury had cytoprotective effects (132).

Although most APPs play a role in preserving tissue integrity, some of them can also facilitate injury besides protection. For example, fibrinogen can activate immune cells, thereby enhancing inflammation. On the other hand, fibrinogen induces tissue repair as a scaffold protein for tissue regeneration (126,133,134). After ischemia-reperfusion injury renal function and survival was worse in fibrinogen knockout mice (135), although renal fibrogenesis was decreased after unilateral ureteral obstruction (136).

Serum amyloid A is also involved both in proinflammatory and anti-inflammatory processes. It has an ability to enhance proinflammatory cytokine production and attract phagocytes, but it can also promote anti-inflammatory cytokine secretion and

macrophage polarisation to M2 phenotype (125,137). Similarly, both prooxidant and antioxidant activities of ceruloplasmin have been described (117).

Considering the markedly increased production of a great number of APPs in the kidney, they could be of utility as biomarkers too. In support of this, Zager et al. (38) detected elevated haptoglobin concentration in the urine of AKI patients. They also found that LPS-induced upregulation of haptoglobin was greater in the kidneys than in the liver in mice (38). Also, Chil3 and other chitinase-like proteins were described as potential biomarkers of septic AKI in both mice and humans (113).

However, the temporal expression pattern of APPs in septic AKI has to be explored before they can be considered as biomarkers for early detection. Previously very few studies determined changes in APPs at time points other than 24 h after LPS administration. These scarce findings regarding EP showed that haptoglobin was upregulated (38), hemopexin was slightly increased (39), while albumin was unchanged (43) 4 h after endotoxin administration in mice. We determined the temporal expression pattern of many APPs in more detail at 4 different time points. Renal mRNA expression of many APPs was induced already during the EP and peaked at 24 h. Among the APPs studied, gene expression of Lcn-2, ceruloplasmin and haptoglobin was upregulated the earliest, followed by complement C3, fibrinogen-α, -β, -γ, hemopexin, serum amyloid A, inter alpha-trypsin inhibitor heavy chain 4 and ferritin heavy chain at 6 h. Their enhanced mRNA expression resulted in elevated renal protein levels by the established phase of AKI at 24 h. Only the protein concentration of ferritin heavy chain increased already in EP. Transferrin was induced slightly later, as both its mRNA and protein expression was elevated first at LP24h. The decrease in the gene expression of fibrinogens, ceruloplasmin, hemopexin, serum amyloid A and ferritin heavy chain by 48 h, suggests that recovery was initiated. At the same time, renal mRNA expression of the negative APP, albumin was suppressed by LPS during LP.

The renal protein concentration of serine protease inhibitor A3K and alpha-1-antitrypsin isoforms Serpina1a and 1c was not increased because of local induction of their mRNA expression. It can be assumed that they may be of hepatic origin, since e.g. serine protease inhibitor A3K is a liver-specific gene (138).

6. Conclusions

The major findings of this study are the following:

- Bacterial lipopolysaccharide (LPS) administration caused serious septic AKI characterized by severe functional impairment of the kidney, upregulation of several inflammatory markers, and marked changes in the expression of regulatory microRNAs (miRNAs) and large number of proteins. Both the renal miRNome and proteome changes were modest at 1.5 h and peaked at 6 and 24 h after LPS-administration. Recovery could be detected at 48 h.
- MiRNA microarray indicated that 71 miRNAs changed significantly at 1.5 and 6 h and 39 at 24 and 48 h. Expression of miR-762 was most upregulated at 6 h after LPS administration and is a newly identified miRNA that is upregulated in septic AKI. MiR-762 and other upregulated miRNAs may play a protective role against renal inflammation by attenuating the LPS-induced immune response.
- Based on our present results we assume that aquaporin-1 (Aqp1) and solute carrier family 22 member 8 (Slc22a8) are regulated by miR-144-3p. Furthermore, the electrogenic sodium bicarbonate cotransporter 1 (Slc4a4 or NBCe1) could be a possible target of miR-144-3p and miR-223-3p. Our data support a pathogenic role for these transporters in LPS-induced AKI.
- Acute-phase proteins (APPs) were among the significantly upregulated proteins. APPs were produced locally in the kidney as demonstrated by renal mRNA expression of most detected APPs, suggesting that a local acute phase reaction is also a characteristic response of the kidney to massive systemic inflammation.

7. Summary

Bacterial lipopolysaccharide-induced systemic inflammation and circulatory shock is associated with acute kidney injury (AKI). We investigated the temporal changes in renal miRNA and protein expression induced by endotoxin shock in mice.

AKI was induced in male outbred NMRI mice by intraperitoneal LPS injections. Mice were sacrificed at 1.5 and 6 h (early phase, EP) or at 24 and 48 h (late phase, LP) after LPS injection. The temporal miRNome profile of septic AKI was established using miRCURY LNA™ miRNA microarray and verified by qPCR. Total renal proteome was analysed by HPLC-MS/MS.

AKI was confirmed by increased plasma urea concentrations and enhanced renal mRNA expression of IL-6, Tnf-α and Lcn-2. Renal miRNome and proteome changes were mild at 1.5 h. We detected the strongest miRNA dysregulation at 6 and 24 h that started to normalize by 48 h. In EP, miR-762 was the most upregulated miRNA that we newly associated with septic AKI. A predicted target of miR-762, Ras related GTPase 1B (Sar1b) was downregulated, indicating that miR-762 may regulate GTP signalling. In LP, miR-21a-5p was the most induced miRNA followed by miR-144-3p, miR-146a-5p and miR-451a. Renal protein concentration of potential protein targets of miR-144-3p was downregulated in LP, which were: aquaporin-1 (Aqp1), solute carrier family 22 member 8 (Slc22a8 or Oat3) and electrogenic sodium bicarbonate cotransporter 1 (Slc4a4 or NBCe1). These miRNAs and transporters may play an important role in LPS-induced AKI and renal inflammation.

As part of the renal inflammation induced by LPS, we demonstrated a massive, complex and coordinated local acute-phase response (APR) of the kidney. APPs dominated the proteome in LP (the ratio of APPs among proteins upregulated at least 4-fold was: EP, 1.5 h: 0/10, 6 h: 1/10; LP, 24 h: 22/47, 48 h: 17/44). Lipocalin-2, complement C3, fibrinogen, haptoglobin and hemopexin were the most upregulated APPs. Renal mRNA expression of APPs was measured by qPCR. The mRNA expression of APPs was induced in EP, preceding the changes in protein concentrations, and confirming local renal production of most APPs.

8. References

1. Kempker JA, Martin GS. The Changing Epidemiology and Definitions of Sepsis. Clin Chest Med [Internet]. 2016;37:165–179. doi: 10.1016/j.ccm.2016.01.002. Cited: in: : PMID: 27229635.
2. Wittebole X, Szakmany T, Lupu M-N, Lipman J, Leone M, Ñamendys-Silva SA, Vincent J-L, Martin-Loeches I, Sakr Y, Jaschinski U. Sepsis in intensive care unit patients: worldwide data from the Intensive Care over Nations Audit. Open Forum Infect Dis. 2018;5:1–9. doi: 10.1093/ofid/ofy313. Cited: in: : PMID: 30555852.
3. Singer M, Deutschman CS, Seymour C, Shankar-Hari M, Annane D, Bauer M, Bellomo R, Bernard GR, Chiche JD, Coopersmith CM, et al. The third international consensus definitions for sepsis and septic shock (sepsis-3). JAMA - J Am Med Assoc. 2016;315:801–810. doi: 10.1001/jama.2016.0287. Cited: in: : PMID: 26903338.
4. Ma S, Evans RG, Iguchi N, Tare M, Parkington HC, Bellomo R, May CN, Lankadeva YR. Sepsis-induced acute kidney injury: A disease of the microcirculation. Microcirculation [Internet]. 2018;e12483. doi: 10.1111/micc.12483. Cited: in: : PMID: 29908046.
5. Mårtensson J, Bellomo R. Sepsis-induced acute kidney injury. Crit Care Clin [Internet]. 2015;31:649–660. doi: 10.1016/j.ccc.2015.06.003. Cited: in: : PMID: 26410135.
6. Makris K, Spanou L. Acute Kidney Injury: Definition, Pathophysiology and Clinical Phenotypes. Clin Biochem Rev [Internet]. 2016;37:85–98. Cited: in: : PMID: 28303073.
7. Gomez H, Ince C, De Backer D, Pickkers P, Payen D, Hotchkiss J, Kellum JA. A unified theory of sepsis-induced acute kidney injury: inflammation, microcirculatory dysfunction, bioenergetics, and the tubular cell adaptation to injury. Shock [Internet]. 2014;41:3–11. doi: 10.1097/SHK.0000000000000052. Cited: in: : PMID: 24346647.
8. Doi K, Leelahavanichkul A, Yuen PST, Star RA. Animal models of sepsis and sepsis-induced kidney injury. J Clin Invest [Internet]. 2009;119:2868–2878. doi: 10.1172/JCI39421. Cited: in: : PMID: 19805915.
9. Lilley E, Armstrong R, Clark N, Gray P, Hawkins P, Mason K, López-Salesansky

N, Stark AK, Jackson SK, Thiemermann C, et al. Refinement of animal models of sepsis and septic shock. Shock. 2015;43:304–316. doi: 10.1097/SHK.0000000000000318. Cited: in: : PMID: 25565638.

10. Fani F, Regolisti G, Delsante M, Cantaluppi V, Castellano G, Gesualdo L, Villa G, Fiaccadori E. Recent advances in the pathogenetic mechanisms of sepsis-associated acute kidney injury. J Nephrol [Internet]. 2017;31:351–359. doi: 10.1007/s40620-017-0452-4. Cited: in: : PMID: 29273917.
11. Beutler B, Rietschel ET. Innate immune sensing and its roots: The story of endotoxin. Nat Rev Immunol. 2003;3:169–176. doi: 10.1038/nri1004.
12. Kellum JA, Prowle JR. Paradigms of acute kidney injury in the intensive care setting. Nat Rev Nephrol [Internet]. 2018;14:217–230. doi: 10.1038/nrneph.2017.184. Cited: in: : PMID: 29355173.
13. Heemann U, Szabo A, Hamar P, Müller V, Witzke O, Lutz J, Philipp T. Lipopolysaccharide pretreatment protects from renal ischemia/reperfusion injury : possible connection to an interleukin-6-dependent pathway. Am J Pathol [Internet]. 2000;156:287–293. doi: 10.1016/S0002-9440(10)64729-3. Cited: in: : PMID: 10623677.
14. Ferrara G, Kanoore Edul VS, Caminos Eguillor JF, Buscetti MG, Canales HS, Lattanzio B, Gatti L, Ince C, Dubin A. Effects of fluid and norepinephrine resuscitation in a sheep model of endotoxin shock and acute kidney injury. J Appl Physiol [Internet]. 2019;127:788–797. doi: 10.1152/japplphysiol.00172.2019. Cited: in: : PMID: 31295071.
15. Lugon JR, Boim MA, Ramos OL, Ajzen H, Schor N. Renal function and glomerular hemodynamics in male endotoxemic rats. Kidney Int [Internet]. 1989;36:570–575. doi: 10.1038/ki.1989.232. Cited: in: : PMID: 2681930.
16. Knotek M, Rogachev B, Wang W, Ecder T, Melnikov V, Gengaro PE, Esson M, Edelstein CL, Dinarello CA, Schrier RW. Endotoxemic renal failure in mice: Role of tumor necrosis factor independent of inducible nitric oxide synthase. Kidney Int [Internet]. 2001;59:2243–2249. doi: 10.1046/j.1523-1755.2001.00740.x. Cited: in: : PMID: 11380827.
17. Cohen RI, Hassell AM, Marzouk K, Marini C, Liu SF, Scharf SM. Renal effects of nitric oxide in endotoxemia. Am J Respir Crit Care Med [Internet].

2001;164:1890–1895. doi: 10.1164/ajrccm.164.10.2103140. Cited: in: : PMID: 11734442.

18. Kaucsár T, Bodor C, Godó M, Szalay C, Révész C, Németh Z, Mózes M, Szénási G, Rosivall L, Soti C, et al. LPS-induced delayed preconditioning is mediated by Hsp90 and involves the heat shock response in mouse kidney. PLoS One. 2014;9:1–7. doi: 10.1371/journal.pone.0092004. Cited: in: : PMID: 24646925.
19. Tod P, Róka B, Kaucsár T, Szatmári K, Vizovišek M, Vidmar R, Fonovič M, Szénási G, Hamar P. Time-Dependent miRNA Profile during Septic Acute Kidney Injury in Mice. Int J Mol Sci [Internet]. 2020;21:5316. doi: 10.3390/ijms21155316.
20. Róka B, Tod P, Kaucsár T, Vizovišek M, Vidmar R, Turk B, Fonović M, Szénási G, Hamar P. The Acute Phase Response Is a Prominent Renal Proteome Change in Sepsis in Mice. Int J Mol Sci [Internet]. 2020;21:200. doi: 10.3390/ijms21010200. Cited: in: : PMID: 31892161.
21. Gabay C, Kushner I. Acute-phase proteins and other systemic responses to inflammation. Epstein FH, editor. N Engl J Med [Internet]. 1999;340:448–454. doi: 10.1056/NEJM199902113400607. Cited: in: : PMID: 9971870.
22. Moshage H. Cytokines and the hepatic acute phase response. J Pathol. 1997;181:257–266. doi: 10.1002/(SICI)1096-9896(199703)181:3<257::AID-PATH756>3.0.CO;2-U. Cited: in: : PMID: 9155709.
23. Schrödl W, Büchler R, Wendler S, Reinhold P, Muckova P, Reindl J, Rhode H. Acute phase proteins as promising biomarkers: Perspectives and limitations for human and veterinary medicine. Proteomics - Clin Appl. 2016;10:1077–1092. doi: 10.1002/prca.201600028. Cited: in: : PMID: 27274000.
24. Henriquez-Camacho C, Losa J. Biomarkers for sepsis. Biomed Res Int. 2014;2014. doi: 10.1155/2014/547818. Cited: in: : PMID: 24800240.
25. Kaucsár T, Godó M, Révész C, Kovács M, Mócsai A, Kiss N, Albert M, Krenács T, Szénási G, Hamar P. Urine/plasma neutrophil gelatinase associated lipocalin ratio is a sensitive and specific marker of subclinical acute kidney injury in mice. PLoS One. 2016;11:1–16. doi: 10.1371/journal.pone.0148043. Cited: in: : PMID: 26824608.
26. Chakraborty S, Kaur S, Guha S, Batra SK. The multifaceted roles of neutrophil gelatinase associated lipocalin (NGAL) in inflammation and cancer. Biochim

Biophys Acta [Internet]. 2012;1826:129–169. doi: 10.1016/j.bbcan.2012.03.008. Cited: in: : PMID: 22513004.

27. Zyłka A, Gala-Błądzińska A, Dumnicka P, Ceranowicz P, Kuźniewski M, Gil K, Olszanecki R, Kuśnierz-Cabala B. Is Urinary NGAL Determination Useful for Monitoring Kidney Function and Assessment of Cardiovascular Disease? A 12-Month Observation of Patients with Type 2 Diabetes. Dis Markers. 2016;2016. doi: 10.1155/2016/8489543.
28. Sporek M, Gala-Błądzińska A, Dumnicka P, Mazur-Laskowska M, Kielczewski S, Walocha J, Ceranowicz P, Kuźniewski M, Mituś J, Kuśnierz-Cabala B. Urine NGAL is useful in the clinical evaluation of renal function in the early course of acute pancreatitis. Folia Med Cracov. 2016;56:13–25. Cited: in: : PMID: 27513835.
29. Schrezenmeier E V., Barasch J, Budde K, Westhoff T, Schmidt-Ott KM. Biomarkers in acute kidney injury – pathophysiological basis and clinical performance. Acta Physiol. 2017;219:554–572. doi: 10.1111/apha.12764. Cited: in: : PMID: 27474473.
30. Sporek M, Dumnicka P, Gala-Błądzińska A, Mazur-Laskowska M, Walocha J, Ceranowicz P, Warzecha Z, Dembiński A, Kuźniewski M, Olszanecki R, et al. Determination of serum neutrophil gelatinase-associated lipocalin at the early stage of acute pancreatitis. Folia Med Cracov. 2016;56:5–16. Cited: in: : PMID: 28013317.
31. Thorsvik S, Bakke I, van Beelen Granlund A, Røyset ES, Damås JK, Østvik AE, Sandvik AK. Expression of neutrophil gelatinase-associated lipocalin (NGAL) in the gut in Crohn's disease. Cell Tissue Res [Internet]. 2018;374:339–348. doi: 10.1007/s00441-018-2860-8. Cited: in: : PMID: 29869714.
32. Buonafine M, Martinez-Martinez E, Jaisser F ric. More than a simple biomarker: The role of NGAL in cardiovascular and renal diseases. Clin Sci. 2018;132:909–923. doi: 10.1042/CS20171592. Cited: in: : PMID: 29739822.
33. Wajda J, Dumnicka P, Maraj M, Ceranowicz P, Kuźniewski M, Kuśnierz-Cabala B. Potential prognostic markers of acute kidney injury in the early phase of acute pancreatitis. Int J Mol Sci. 2019;20:1–20. doi: 10.3390/ijms20153714.
34. Bascands JL, Bachvarova M, Neau E, Schanstra JP, Bachvarov D. Molecular

determinants of LPS-induced acute renal inflammation: Implication of the kinin B1receptor. Biochem Biophys Res Commun [Internet]. 2009;386:407–412. doi: 10.1016/j.bbrc.2009.06.063. Cited: in: : PMID: 19538936.

35. Kalmovarin N, Friedrichs WE, O'Brien H V, Linehan LA, Bowman BH, Yang F. Extrahepatic expression of plasma protein genes during inflammation. Inflammation [Internet]. 1991;15:369–379. Cited: in: : PMID: 1757124.
36. Baumann H, Wang Y, Richards CD, Jones CA, Black TA, Gross KW. Endotoxin-induced renal inflammatory response: Oncostatin M as a major mediator of suppressed renin expression. J Biol Chem. 2000;275:22014–22019. doi: 10.1074/jbc.M002830200. Cited: in: : PMID: 10806209.
37. D'Armiento J, Dalal SS, Chada K. Tissue, temporal and inducible expression pattern of haptoglobin in mice. Gene [Internet]. 1997;195:19–27. Cited: in: : PMID: 9300815.
38. Zager RA, Vijayan A, Johnson ACM. Proximal tubule haptoglobin gene activation is an integral component of the acute kidney injury "stress response." Am J Physiol Physiol [Internet]. 2012;303:F139–F148. doi: 10.1152/ajprenal.00168.2012.
39. Zager RA, Johnson ACM, Becker K. Renal cortical hemopexin accumulation in response to acute kidney injury. AJP Ren Physiol [Internet]. 2012;303:F1460–F1472. doi: 10.1152/ajprenal.00426.2012. Cited: in: : PMID: 22993068.
40. Ault BH, Colten HR. Cellular specificity of murine renal C3 expression in two models of inflammation. Immunology. 1994;81:655–660. Cited: in: : PMID: 8039815.
41. Cunningham PN, Holers VM, Alexander JJ, Guthridge JM, Carroll MC, Quigg RJ. Complement is activated in kidney by endotoxin but does not cause the ensuing acute renal failure. Kidney Int. 2000;58:1580–1587. doi: 10.1046/j.1523-1755.2000.00319.x. Cited: in: : PMID: 11012892.
42. Gupta KK, Donahue DL, Sandoval-Cooper MJ, Castellino FJ, Ploplis VA. Abrogation of plasminogen activator inhibitor-1-vitronectin interaction ameliorates acute kidney injury in murine endotoxemia. PLoS One. 2015;10:1–20. doi: 10.1371/journal.pone.0120728.
43. Ware LB, Johnson ACM, Zager RA. Renal cortical albumin gene induction and urinary albumin excretion in response to acute kidney injury. Am J Physiol Renal

Physiol [Internet]. 2011;300:F628-38. doi: 10.1152/ajprenal.00654.2010. Cited: in: : PMID: 21147844.

44. Kaucsár T, Rácz Z, Hamar P. Post-transcriptional gene-expression regulation by micro RNA (miRNA) network in renal disease. Adv Drug Deliv Rev. 2010;62:1390–1401. doi: 10.1016/j.addr.2010.10.003.

45. Ren G, Zhu J, Li J, Meng X. Noncoding RNAs in acute kidney injury. J Cell Physiol [Internet]. 2019;234:2266–2276. doi: 10.1002/jcp.27203. Cited: in: : PMID: 30146769.

46. Brandenburger T, Lorenzen JM. Diagnostic and Therapeutic Potential of microRNAs in Acute Kidney Injury. Front Pharmacol [Internet]. 2020;11:657. doi: 10.3389/fphar.2020.00657. Cited: in: : PMID: 32477132.

47. Qi J, Qiao Y, Wang P, Li S, Zhao W, Gao C. MicroRNA-210 negatively regulates LPS-induced production of proinflammatory cytokines by targeting NF-κB1 in murine macrophages. FEBS Lett [Internet]. 2012;586:1201–1207. doi: 10.1016/j.febslet.2012.03.011.

48. Jiang Q, Wu C, Zhang Q. [microRNA-34a participates in lipopolysaccharide mediated sepsis related renal function impairment via Kruppel-like factor 4]. Zhonghua Wei Zhong Bing Ji Jiu Yi Xue [Internet]. 2018;30:351–354. doi: 10.3760/cma.j.issn.2095-4352.2018.04.013. Cited: in: : PMID: 29663998.

49. Fu D, Dong J, Li P, Tang C, Cheng W, Xu Z, Zhou W, Ge J, Xia C, Zhang Z. MiRNA-21 has effects to protect kidney injury induced by sepsis. Biomed Pharmacother [Internet]. 2017;94:1138–1144. doi: 10.1016/j.biopha.2017.07.098.

50. Taganov KD, Boldin MP, Chang KJ, Baltimore D. NF-κB-dependent induction of microRNA miR-146, an inhibitor targeted to signaling proteins of innate immune responses. Proc Natl Acad Sci U S A. 2006;103:12481–12486. doi: 10.1073/pnas.0605298103. Cited: in: : PMID: 16885212.

51. Colbert JF, Ford JA, Haeger SM, Yang Y, Dailey KL, Allison KC, Neudecker V, Evans CM, Richardson VL, Brodsky KS, et al. A model-specific role of microRNA-223 as a mediator of kidney injury during experimental sepsis. Am J Physiol Physiol. 2017;313:F553–F559. doi: 10.1152/ajprenal.00493.2016.

52. Ding Y, Guo F, Zhu T, Li J, Gu D, Jiang W, Lu Y, Zhou D. Mechanism of long non-coding RNA MALAT1 in lipopolysaccharide-induced acute kidney injury is

mediated by the miR-146a/NF-κB signaling pathway. Int J Mol Med. 2018;41:446–454. doi: 10.3892/ijmm.2017.3232.

53. Ikeda S, Yamamoto H, Masuda M, Takei Y, Nakahashi O, Kozai M, Tanaka S, Nakao M, Taketani Y, Segawa H, et al. Downregulation of renal type IIa sodium-dependent phosphate cotransporter during lipopolysaccharide-induced acute inflammation. Am J Physiol Physiol [Internet]. 2014;306:F744–F750. doi: 10.1152/ajprenal.00474.2013. Cited: in: : PMID: 24500689.

54. Edgar R, Domrachev M, Lash AE. Gene Expression Omnibus: NCBI gene expression and hybridization array data repository. Nucleic Acids Res [Internet]. 2002;30:207–210. doi: 10.1093/nar/30.1.207. Cited: in: : PMID: 11752295.

55. Andersen CL, Jensen JL, Ørntoft TF. Normalization of real-time quantitative reverse transcription-PCR data: a model-based variance estimation approach to identify genes suited for normalization, applied to bladder and colon cancer data sets. Cancer Res [Internet]. 2004;64:5245–5250. doi: 10.1158/0008-5472.CAN-04-0496. Cited: in: : PMID: 15289330.

56. Vidmar R, Vizovišek M, Turk D, Turk B, Fonović M. Protease cleavage site fingerprinting by label-free in-gel degradomics reveals pH-dependent specificity switch of legumain. EMBO J [Internet]. 2017;e201796750. doi: 10.15252/embj.201796750. Cited: in: : PMID: 28733325.

57. Sobotič B, Vizovišek M, Vidmar R, Van Damme P, Gocheva V, Joyce JA, Gevaert K, Turk V, Turk B, Fonović M. Proteomic Identification of Cysteine Cathepsin Substrates Shed from the Surface of Cancer Cells. Mol Cell Proteomics [Internet]. 2015;14:2213–2228. doi: 10.1074/mcp.M114.044628. Cited: in: : PMID: 26081835.

58. Cox J, Mann M. MaxQuant enables high peptide identification rates, individualized p.p.b.-range mass accuracies and proteome-wide protein quantification. Nat Biotechnol. 2008;26:1367–1372. doi: 10.1038/nbt.1511.

59. Deutsch EW, Csordas A, Sun Z, Jarnuczak A, Perez-Riverol Y, Ternent T, Campbell DS, Bernal-Llinares M, Okuda S, Kawano S, et al. The ProteomeXchange consortium in 2017: supporting the cultural change in proteomics public data deposition. Nucleic Acids Res. 2017;45:D1100–D1106. doi: 10.1093/nar/gkw936.

60. Chou C-H, Shrestha S, Yang C-D, Chang N-W, Lin Y-L, Liao K-W, Huang W-C, Sun T-H, Tu S-J, Lee W-H, et al. miRTarBase update 2018: a resource for experimentally validated microRNA-target interactions. Nucleic Acids Res [Internet]. 2018;46:D296–D302. doi: 10.1093/nar/gkx1067. Cited: in: : PMID: 29126174.
61. Chen Y, Wang X. miRDB: an online database for prediction of functional microRNA targets. Nucleic Acids Res [Internet]. 2020;48:D127–D131. doi: 10.1093/nar/gkz757.
62. Liu W, Wang X. Prediction of functional microRNA targets by integrative modeling of microRNA binding and target expression data. Genome Biol [Internet]. 2019;20:18. doi: 10.1186/s13059-019-1629-z.
63. Betel D, Wilson M, Gabow A, Marks DS, Sander C. The microRNA.org resource: targets and expression. Nucleic Acids Res [Internet]. 2007;36:D149–D153. doi: 10.1093/nar/gkm995.
64. Zager RA, Johnson ACM, Frostad KB. Rapid renal alpha-1 antitrypsin gene induction in experimental and clinical acute kidney injury. PLoS One. 2014;9. doi: 10.1371/journal.pone.0098380. Cited: in: : PMID: 24848503.
65. Motulsky HJ, Brown RE. Detecting outliers when fitting data with nonlinear regression - a new method based on robust nonlinear regression and the false discovery rate. BMC Bioinformatics [Internet]. 2006;7:123. doi: 10.1186/1471-2105-7-123. Cited: in: : PMID: 16526949.
66. Benovoy D, Kwan T, Majewski J. Effect of polymorphisms within probe-target sequences on olignonucleotide microarray experiments. Nucleic Acids Res. 2008;36:4417–4423. doi: 10.1093/nar/gkn409.
67. Tsai CA, Hsueh HM, Chen JJ. Estimation of False Discovery Rates in Multiple Testing: Application to Gene Microarray Data. Biometrics. 2003;59:1071–1081. doi: 10.1111/j.0006-341X.2003.00123.x.
68. Pawitan Y, Michiels S, Koscielny S, Gusnanto A, Ploner A. False discovery rate, sensitivity and sample size for microarray studies. Bioinformatics. 2005;21:3017–3024. doi: 10.1093/bioinformatics/bti448.
69. Wright GW, Simon RM. A random variance model for detection of differential gene expression in small microarray experiments. Bioinformatics. 2003;19:2448–

2455. doi: 10.1093/bioinformatics/btg345.

70. Reiner A, Yekutieli D, Benjamini Y. Identifying differentially expressed genes using false discovery rate controlling procedures. Bioinformatics. 2003;19:368–375. doi: 10.1093/bioinformatics/btf877. Cited: in: : PMID: 12584122.

71. Ueno K, Samura M, Nakamura T, Tanaka Y, Takeuchi Y, Kawamura D, Takahashi M, Hosoyama T, Morikage N, Hamano K. Increased plasma VEGF levels following ischemic preconditioning are associated with downregulation of miRNA-762 and miR-3072-5p. Sci Rep. 2016;6:1–9. doi: 10.1038/srep36758.

72. Takai Y, Sasaki T, Matozaki T. Small GTP-binding proteins. Physiol Rev [Internet]. 2001;81:153–208. doi: 10.1152/physrev.2001.81.1.153. Cited: in: : PMID: 11152757.

73. Sané A, Ahmarani L, Delvin E, Auclair N, Spahis S, Levy E. SAR1B GTPase is necessary to protect intestinal cells from disorders of lipid homeostasis, oxidative stress, and inflammation. J Lipid Res. 2019;60:1755–1764. doi: 10.1194/jlr.RA119000119. Cited: in: : PMID: 31409740.

74. Li Y, Huang R, Wang L, Hao J, Zhang Q, Ling R, Yun J. microRNA-762 promotes breast cancer cell proliferation and invasion by targeting IRF7 expression. Cell Prolif. 2015;48:643–649. doi: 10.1111/cpr.12223.

75. Zhang X, Wang X, Zhu H, Zhu C, Wang Y, Pu WT, Jegga AG, Fan GC. Synergistic effects of the GATA-4-mediated miR-144/451 cluster in protection against simulated ischemia/reperfusion-induced cardiomyocyte death. J Mol Cell Cardiol [Internet]. 2010;49:841–850. doi: 10.1016/j.yjmcc.2010.08.007.

76. Xu P, Palmer LE, Lechauve C, Zhao G, Yao Y, Luan J, Vourekas A, Tan H, Peng J, Schuetz JD, et al. Regulation of gene expression by miR-144/451 during mouse erythropoiesis. Blood. 2019;133:2518–2528. doi: 10.1182/blood.2018854604.

77. Li J, Rohailla S, Gelber N, Rutka J, Sabah N, Gladstone RA, Wei C, Hu P, Kharbanda RK, Redington AN. MicroRNA-144 is a circulating effector of remote ischemic preconditioning. Basic Res Cardiol. 2014;109. doi: 10.1007/s00395-014-0423-z.

78. Fan G, Jiang X, Wu X, Fordjour PA, Miao L, Zhang H, Zhu Y, Gao X. Anti-Inflammatory Activity of Tanshinone IIA in LPS-Stimulated RAW264.7 Macrophages via miRNAs and TLR4–NF-κB Pathway. Inflammation.

2016;39:375–384. doi: 10.1007/s10753-015-0259-1.

79. Li H, Shi H, Gao M, Ma N, Sun R. Long non-coding RNA CASC2 improved acute lung injury by regulating miR-144-3p/AQP1 axis to reduce lung epithelial cell apoptosis. Cell Biosci [Internet]. 2018;8:1–11. doi: 10.1186/s13578-018-0205-7.
80. Yu G, Liu Q, Dong X, Tang K, Li B, Liu C, Zhang W, Wang Y, Jin Y. Inhibition of inflammation using diacerein markedly improved renal function in endotoxemic acute kidney injured mice. Cell Mol Biol Lett. 2018;23:1–12. doi: 10.1186/s11658-018-0107-z.
81. Li B, Liu C, Tang K, Dong X, Xue L, Su G, Zhang W, Jin Y. Aquaporin-1 attenuates macrophage-mediated inflammatory responses by inhibiting p38 mitogen-activated protein kinase activation in lipopolysaccharide-induced acute kidney injury. Inflamm Res [Internet]. 2019;68:1035–1047. doi: 10.1007/s00011-019-01285-1.
82. Li B, Liu C, Tang K, Dong X, Xue L, Su G, Zhang W, Jin Y. Aquaporin-1 attenuates macrophage-mediated inflammatory responses by inhibiting p38 mitogen-activated protein kinase activation in lipopolysaccharide-induced acute kidney injury. Inflamm Res. 2019;68:1035–1047. doi: 10.1007/s00011-019-01285-1.
83. Kieran NE, Doran PP, Connolly SB, Greenan MC, Higgins DF, Leonard M, Godson C, Taylor CT, Henger A, Kretzler M, et al. Modification of the transcriptomic response to renal ischemia/reperfusion injury by lipoxin analog. Kidney Int. 2003;64:480–492. doi: 10.1046/j.1523-1755.2003.00106.x.
84. Asvapromtada S, Sonoda H, Kinouchi M, Oshikawa S, Takahashi S, Hoshino Y, Sinlapadeelerdkul T, Yokota-Ikeda N, Matsuzaki T, Ikeda M. Characterization of urinary exosomal release of aquaporin-1 and -2 after renal ischemia-reperfusion in rats. Am J Physiol Physiol [Internet]. 2018;314:F584–F601. doi: 10.1152/ajprenal.00184.2017.
85. Wang W, Li C, Summer SN, Falk S, Wang W, Ljubanovic D, Schrier RW. Role of AQP1 in endotoxemia-induced acute kidney injury. Am J Physiol - Ren Physiol. 2008;294:1473–1480. doi: 10.1152/ajprenal.00036.2008.
86. Wang Y, Zhang W, Yu G, Liu Q, Jin Y. Cytoprotective effect of aquaporin 1 against lipopolysaccharide-induced apoptosis and inflammation of renal epithelial

hk-2 cells. Exp Ther Med. 2018;15:4243–4252. doi: 10.3892/etm.2018.5992.

87. Höcherl K, Schmidt C, Bucher M. COX-2 inhibition attenuates endotoxin-induced downregulation of organic anion transporters in the rat renal cortex. Kidney Int [Internet]. 2009;75:373–380. doi: 10.1038/ki.2008.557.

88. Huh Y, Keep RF, Smith DE. Impact of Lipopolysaccharide-Induced Inflammation on the Disposition of the Aminocephalosporin Cefadroxil. Antimicrob Agents Chemother [Internet]. 2013;57:6171–6178. doi: 10.1128/AAC.01497-13.

89. Kaucsár T, Révész C, Godó M, Krenács T, Albert M, Szalay CI, Rosivall L, Benyó Z, Bátkai S, Thum T, et al. Activation of the miR-17 Family and miR-21 During Murine Kidney Ischemia-Reperfusion Injury. Nucleic Acid Ther. 2013;23:344–354. doi: 10.1089/nat.2013.0438.

90. Pan T, Jia P, Chen N, Fang Y, Liang Y, Guo M, Ding X. Delayed remote ischemic preconditioning confers renoprotection against septic acute kidney injury via exosomal miR-21. Theranostics. 2019;9:405–423. doi: 10.7150/thno.29832.

91. Jia P, Wu X, Dai Y, Teng J, Fang Y, Hu J, Zou J, Liang M, Ding X. MicroRNA-21 Is Required for Local and Remote Ischemic Preconditioning in Multiple Organ Protection Against Sepsis. Crit Care Med. 2017;45:e703–e710. doi: 10.1097/CCM.0000000000002363.

92. Boldin MP, Taganov KD, Rao DS, Yang L, Zhao JL, Kalwani M, Garcia-Flores Y, Luong M, Devrekanli A, Xu J, et al. miR-146a is a significant brake on autoimmunity, myeloproliferation, and cancer in mice. J Exp Med. 2011;208:1189–1201. doi: 10.1084/jem.20101823.

93. Wu R, Su Y, Wu H, Dai Y, Zhao M, Lu Q. Characters, functions and clinical perspectives of long non-coding RNAs. Mol Genet Genomics. 2016;291:1013–1033. doi: 10.1007/s00438-016-1179-y.

94. Johnnidis JB, Harris MH, Wheeler RT, Stehling-Sun S, Lam MH, Kirak O, Brummelkamp TR, Fleming MD, Camargo FD. Regulation of progenitor cell proliferation and granulocyte function by microRNA-223. Nature [Internet]. 2008;451:1125–1129. doi: 10.1038/nature06607.

95. Wang J, Yu M, Yu G, Bian J, Deng X, Wan X, Zhu K. Serum miR-146a and miR-223 as potential new biomarkers for sepsis. Biochem Biophys Res Commun [Internet]. 2010;394:184–188. doi: 10.1016/j.bbrc.2010.02.145.

96. Yu C-H, Xu C-F, Li Y-M. Association of MicroRNA-223 Expression with Hepatic Ischemia/Reperfusion Injury in Mice. Dig Dis Sci [Internet]. 2009;54:2362–2366. doi: 10.1007/s10620-008-0629-8.
97. Wang J, Bai X, Song Q, Fan F, Hu Z, Cheng G, Zhang Y. miR-223 inhibits lipid deposition and inflammation by suppressing toll-like receptor 4 signaling in macrophages. Int J Mol Sci. 2015;16:24965–24982. doi: 10.3390/ijms161024965.
98. Wang X, Huang W, Yang Y, Wang Y, Peng T, Chang J, Caldwell CC, Zingarelli B, Fan GC. Loss of duplexmiR-223 (5p and 3p) aggravates myocardial depression and mortality in polymicrobial sepsis. Biochim Biophys Acta - Mol Basis Dis [Internet]. 2014;1842:701–711. doi: 10.1016/j.bbadis.2014.01.012. Cited: in: : PMID: 24486439.
99. Xiao W, Wang X, Wang T, Xing J. MiR-223-3p promotes cell proliferation and metastasis by downregulating SLC4A4 in clear cell renal cell carcinoma. Aging (Albany NY) [Internet]. 2019;11:615–633. doi: 10.18632/aging.101763.
100. Markanday A. Acute phase reactants in infections: evidence-based review and a guide for clinicians. Open forum Infect Dis [Internet]. 2015;2:ofv098. doi: 10.1093/ofid/ofv098. Cited: in: : PMID: 26258155.
101. Koorts AM, Viljoen M. Ferritin and ferritin isoforms I: Structure-function relationships, synthesis, degradation and secretion. Arch Physiol Biochem. 2007;113:30–54. doi: 10.1080/13813450701318583.
102. Tolosano E, Altruda F. Hemopexin: structure, function, and regulation. DNA Cell Biol [Internet]. 2002;21:297–306. doi: 10.1089/104454902753759717. Cited: in: : PMID: 12042069.
103. Linder MC. Ceruloplasmin and other copper binding components of blood plasma and their functions: An update. Metallomics [Internet]. 2016;8:887–905. doi: 10.1039/c6mt00103c. Cited: in: : PMID: 27426697.
104. Leitner DF, Connor JR. Functional roles of transferrin in the brain. Biochim Biophys Acta - Gen Subj [Internet]. 2012;1820:393–402. doi: 10.1016/j.bbagen.2011.10.016.
105. Delanghe JR, Speeckaert R, Speeckaert MM. Complement C3 and its polymorphism: Biological and clinical consequences. Pathology. 2014;46:1–10. doi: 10.1097/PAT.0000000000000042.

106. Upragarin N, Landman WJM, Gaastra W, Gruys E. Extrahepatic production of acute phase serum amyloid A. Histol Histopathol. 2005;20:1295–1307.
107. Buchanan JM, Walter CA, Robinson LK, Eddy CA, Yang F, Herbert DC, Adrian EK, Adrian GS, Weaker FJ, Bowman BH. Expression of a human chimeric transferrin gene in senescent transgenic mice reflects the decrease of transferrin levels in aging humans. Biochim Biophys Acta - Gene Struct Expr. 2003;1132:168–176. doi: 10.1016/0167-4781(92)90008-n.
108. Zhang L, Wang M, Kang X, Boontheung P, Li N, Nel AE, Loo JA. Oxidative stress and asthma: proteome analysis of chitinase-like proteins and FIZZ1 in lung tissue and bronchoalveolar lavage fluid. J Proteome Res [Internet]. 2009;8:1631–1638. doi: 10.1021/pr800685h. Cited: in: : PMID: 19714806.
109. Lee CG, Da Silva CA, Dela Cruz CS, Ahangari F, Ma B, Kang M-J, He C, Takyar S, Elias JA. Role of chitin and chitinase/chitinase-like proteins in inflammation, tissue remodeling, and injury. Annu Rev Physiol [Internet]. 2011;73:479–501. doi: 10.1146/annurev-physiol-012110-142250. Cited: in: : PMID: 21054166.
110. Takeuch O, Akira S. Epigenetic control of macrophage polarization. Eur J Immunol. 2011;41:2490–2493. doi: 10.1002/eji.201141792.
111. Cuartero MI, Ballesteros I, Moraga A, Nombela F, Vivancos J, Hamilton JA, Corbí ÁL, Lizasoain I, Moro MA. N2 neutrophils, novel players in brain inflammation after stroke: Modulation by the pparγ agonist rosiglitazone. Stroke. 2013;44:3498–3508. doi: 10.1161/STROKEAHA.113.002470.
112. Benson MD. Acute-phase reactants. Curr Opin Rheumatol. 1989;1:209–214. doi: 10.1097/00002281-198901020-00014.
113. Maddens B, Ghesquière B, Vanholder R, Demon D, Vanmassenhove J, Gevaert K, Meyer E. Chitinase-like proteins are candidate biomarkers for sepsis-induced acute kidney injury. Mol Cell Proteomics [Internet]. 2012;11:M111.013094. doi: 10.1074/mcp.M111.013094. Cited: in: : PMID: 22233884.
114. Bode JG, Albrecht U, Häussinger D, Heinrich PC, Schaper F. Hepatic acute phase proteins - Regulation by IL-6- and IL-1-type cytokines involving STAT3 and its crosstalk with NF-κB-dependent signaling. Eur J Cell Biol [Internet]. 2012;91:496–505. doi: 10.1016/j.ejcb.2011.09.008. Cited: in: : PMID: 22093287.
115. Quaye IK. Haptoglobin, inflammation and disease. Trans R Soc Trop Med Hyg.

2008;102:735–742. doi: 10.1016/j.trstmh.2008.04.010. Cited: in: : PMID: 18486167.

116. Tolosano E, Fagoonee S, Morello N, Vinchi F, Fiorito V. Heme scavenging and the other facets of hemopexin. Antioxid Redox Signal [Internet]. 2010;12:305–320. doi: 10.1089/ars.2009.2787. Cited: in: : PMID: 19650691.
117. Giurgea N, Constantinescu MI, Stanciu R, Suciu S, Muresan A. Ceruloplasmin - acute-phase reactant or endogenous antioxidant? The case of cardiovascular disease. Med Sci Monit [Internet]. 2005;11:RA48-51. Cited: in: : PMID: 15668644.
118. Choi-Miura NH, Takahashi K, Yoda M, Saito K, Hori M, Ozaki H, Mazda T, Tomita M. The novel acute phase protein, IHRP, inhibits actin polymerization and phagocytosis of polymorphonuclear cells. Inflamm Res. 2000;49:305–310. doi: 10.1007/PL00000211. Cited: in: : PMID: 10939621.
119. Mangaraj M, Nanda R, Panda S. Apolipoprotein A-I: a molecule of diverse function. Indian J Clin Biochem. 2016;31:253–259. doi: 10.1007/s12291-015-0513-1. Cited: in: : PMID: 27382195.
120. Zhang H, Wu L-M, Wu J. Cross-talk between apolipoprotein E and cytokines. Mediators Inflamm. 2011;2011:1–10. doi: 10.1155/2011/949072. Cited: in: : PMID: 21772670.
121. Hochepied T, Berger FG, Baumann H, Libert C. α1-acid glycoprotein: An acute phase protein with inflammatory and immunomodulating properties. Cytokine Growth Factor Rev. 2003;14:25–34. doi: 10.1016/S1359-6101(02)00054-0.
122. Gozzelino R, Soares MP. Coupling heme and iron metabolism via ferritin H chain. Antioxid Redox Signal [Internet]. 2014;20:1754–1769. doi: 10.1089/ars.2013.5666. Cited: in: : PMID: 24124891.
123. Gomme PT, McCann KB. Transferrin: structure, function and potential therapeutic actions. Drug Discov Today. 2005;10:267–273. doi: 10.1016/S1359-6446(04)03333-1. Cited: in: : PMID: 15708745.
124. Meier U, Gressner O, Lammert F, Gressner AM. Gc-globulin: Roles in response to injury. Clin Chem. 2006;52:1247–1253. doi: 10.1373/clinchem.2005.065680.
125. Ye RD, Sun L. Emerging functions of serum amyloid A in inflammation. J Leukoc Biol [Internet]. 2015;98:923–929. doi: 10.1189/jlb.3VMR0315-080R. Cited: in: :

PMID: 26130702.

126. Davalos D, Akassoglou K. Fibrinogen as a key regulator of inflammation in disease. Semin Immunopathol. 2012;34:43–62. doi: 10.1007/s00281-011-0290-8. Cited: in: : PMID: 22037947.
127. Mocchegiani E, Costarelli L, Giacconi R, Cipriano C, Muti E, Malavolta M. Zinc-binding proteins (metallothionein and alpha-2 macroglobulin) and immunosenescence. Exp Gerontol [Internet]. 2006;41:1094–1107. doi: 10.1016/j.exger.2006.08.010. Cited: in: : PMID: 17030107.
128. Ehlers MR. Immune-modulating effects of alpha-1 antitrypsin. Biol Chem [Internet]. 2014;395:1187–1193. doi: 10.1515/hsz-2014-0161. Cited: in: : PMID: 24854541.
129. Pham CG, Bubici C, Zazzeroni F, Papa S, Jones J, Alvarez K, Jayawardena S, De Smaele E, Cong R, Beaumont C, et al. Ferritin heavy chain upregulation by NF-κB inhibits TNFα-induced apoptosis by suppressing reactive oxygen species. Cell. 2004;119:529–542. doi: 10.1016/j.cell.2004.10.017. Cited: in: : PMID: 15537542.
130. Zarjou A, Bolisetty S, Joseph R, Traylor A, Apostolov EO, Arosio P, Balla J, Verlander J, Darshan D, Kuhn LC, et al. Proximal tubule h-ferritin mediates iron trafficking in acute kidney injury. J Clin Invest. 2013;123:4423–4434. doi: 10.1172/JCI67867. Cited: in: : PMID: 24018561.
131. Bolisetty S, Zarjou A, Hull TD, Traylor AM, Perianayagam A, Joseph R, Kamal AI, Arosio P, Soares MP, Jeney V, et al. Macrophage and epithelial cell H-ferritin expression regulates renal inflammation. Kidney Int [Internet]. 2015;88:95–108. doi: 10.1038/ki.2015.102.
132. Hatcher HC, Tesfay L, Torti S V., Torti FM. Cytoprotective effect of ferritin H in renal ischemia reperfusion injury. PLoS One. 2015;10:1–15. doi: 10.1371/journal.pone.0138505. Cited: in: : PMID: 26379029.
133. Sutton TA. Alteration of microvascular permeability in acute kidney injury. Microvasc Res [Internet]. 2009;77:4–7. doi: 10.1016/j.mvr.2008.09.004. Cited: in: : PMID: 18938184.
134. Goto T, Fujigaki Y, Sun DF, Yamamoto T, Hishida A. Plasma protein extravasation and vascular endothelial growth factor expression with endothelial nitric oxide synthase induction in gentamicin-induced acute renal failure in rats.

Virchows Arch. 2004;444:362–374. doi: 10.1007/s00428-004-0977-5.

135. Sörensen-Zender I, Rong S, Susnik N, Lange J, Gueler F, Degen JL, Melk A, Haller H, Schmitt R. Role of fibrinogen in acute ischemic kidney injury. Am J Physiol Physiol [Internet]. 2013;305:F777–F785. doi: 10.1152/ajprenal.00418.2012. Cited: in: : PMID: 23804451.

136. Sörensen I, Susnik N, Inhester T, Degen JL, Melk A, Haller H, Schmitt R. Fibrinogen, acting as a mitogen for tubulointerstitial fibroblasts, promotes renal fibrosis. Kidney Int. 2011;80:1035–1044. doi: 10.1038/ki.2011.214. Cited: in: : PMID: 21734641.

137. Zhou H, Chen M, Zhang G, Ye RD. Suppression of lipopolysaccharide-induced inflammatory response by fragments from serum amyloid A. J Immunol [Internet]. 2017;199:1105–1112. doi: 10.4049/jimmunol.1700470. Cited: in: : PMID: 28674180.

138. Horvath AJ, Forsyth SL, Coughlin PB. Expression patterns of murine antichymotrypsin-like genes reflect evolutionary divergence at the Serpina3 locus. J Mol Evol. 2004;59:488–497. doi: 10.1007/s00239-004-2640-9. Cited: in: : PMID: 15638460.

9. Bibliography of the candidate's publications

Publications related to the thesis

1. Tod P, Róka B, Kaucsár T, Szatmári K, Vizovišek M, Vidmar R, Fonovič M, Szénási G, Hamar P. Time-Dependent miRNA Profile during Septic Acute Kidney Injury in Mice. Int J Mol Sci [Internet]. 2020;21:5316. doi: 10.3390/ijms21155316. (IF: 5.924, rank: Q1)
2. Róka B, Tod P, Kaucsár T, Vizovišek M, Vidmar R, Turk B, Fonović M, Szénási G, Hamar P. The Acute Phase Response Is a Prominent Renal Proteome Change in Sepsis in Mice. Int J Mol Sci [Internet]. 2020;21:200. doi: 10.3390/ijms21010200. Cited: in: : PMID: 31892161. (IF: 5.924, rank: Q1)

Publications not related to the thesis

1. Róka B, Tod P, Kaucsár T, Bukosza ÉN, Vörös I, Varga Z V., Petrovich B, Ágg B, Ferdinandy P, Szénási G, et al. Delayed Contralateral Nephrectomy Halted Post-Ischemic Renal Fibrosis Progression and Inhibited the Ischemia-Induced Fibromir Upregulation in Mice. Biomedicines [Internet]. 2021;9:815. doi: 10.3390/biomedicines9070815. (IF: 4.757, rank: Q1)
2. Tod P, Bukosza EN, Róka B, Kaucsár T, Fintha A, Krenács T, Szénási G, Hamar P. Post-Ischemic Renal Fibrosis Progression Is Halted by Delayed Contralateral Nephrectomy: The Involvement of Macrophage Activation. Int J Mol Sci [Internet]. 2020;21:3825. doi: 10.3390/ijms21113825. (IF: 5.924, rank: Q1)
3. Kaucsár T, Róka B, Tod P, Do PT, Hegedűs Z, Szénási G, Hamar P. Divergent regulation of lncRNA expression by ischemia in adult and aging mice. GeroScience [Internet]. 2022;44:429–445. doi: 10.1007/s11357-021-00460-9. Cited: in: : PMID: 34697716. (IF: 7.581, rank: Q1)

10. Acknowledgements

I am very grateful that I was given the opportunity to participate in the doctoral program. I would like to thank to my supervisors that they gave me this chance. I am also very grateful for all their support throughout the years. I am especially grateful that they always respected my needs and we could find good compromises in our cooperation. I am also pleased to work with all other members of my team. I learned a lot from my teammates and colleagues at the Department of Pathopysiology and the Translational Medicine Institute. I would like to say special thanks to Tamás Kaucsár and Pál Tod for training me the methodologies. I am thankful to all other colleagues at the Department and the Institute who supported me. It was a pleasure to work with all of them. I am also grateful to Dr Zoltán Benyó, the director of the Translational Medicine Institute for his support. I would like to also say thanks to Ildikó Virág and Viktória Szabó-Honfi for taking care of the animal facility. Furthermore, I feel honoured for the collaboration with Matej Vizovišek, Robert Vidmar, Boris Turk and Marko Fonović from the Jožef Stefan Institute in Ljubljana on the proteomic studies.

We are very grateful for all the financial support that was granted for us. Our research was funded by the following funds and grants:

- the Hungarian Scientific Research Fund: OTKA SNN-114619 and ANN-110810 (recipient: Péter Hamar),
- the National Research, Development and Innovation Fund of Hungary: NVKP_16-1-2016-0042 (recipient: Péter Hamar),
- the Economic Development and Innovation Operative Program Grant: GINOP 2.3.2-15-2016-00048 (recipient: Péter Hamar),
- the Slovenian Research Agency grants: N1-0031 and P1-0140 (recipient: Boris Turk).

The research was also supported by the EFOP-3.6.3-VEKOP-16-2017-00009 grant. Péter Hamar was a recipient of, and Pál Tod was partially supported from the Kispál Gyula startup grant (300021) of the University of Pécs.

Finally, I would also like to express my gratitude to my family and friends who gave me a lot of support throughout these years.